Biogeosciences Discuss., doi:10.5194/bg-2016-106, 2016
Manuscript under review for journal Biogeosciences
Published: 18 April 2016

Clumped isotopes in near surface atmospheric CO_2 over land, coast and ocean in Taiwan and its vicinity

Amzad H. Laskar[1] and Mao-Chang Liang[1,2,3,4]*

[1]Research Center for Environmental Changes, Academia Sinica, Taipei, Taiwan

[2]Graduate Institute of Astronomy, National Central University, Taiwan

[3]Institute of Astronomy and Astrophysics, Academia Sinica, Taiwan

[4]Department of Physics, University of Houston, USA

*To whom correspondence should be addressed: mcl@rcec.sinica.edu.tw

Phone: (02) 2653-9885 #852

Fax: (02) 2783-3584

Biogeosciences Discuss., doi:10.5194/bg-2016-106, 2016
Manuscript under review for journal Biogeosciences
Published: 18 April 2016

Abstract

Molecules containing two rare isotopes (e.g., $^{13}C^{18}O^{16}O$ in CO_2), called clumped isotopes, are powerful tools to provide an alternative way to independently constrain the sources of CO_2 in the atmosphere because of their unique physical and chemical properties. We present clumped isotope data (Δ_{47}) in near surface atmospheric CO_2 from urban, sub-urban, ocean, coast, high mountain (~3.3 km a.s.l.) and forest in Taiwan and its vicinity. The primary goal of the study is to use the unique Δ_{47} signature in air CO_2 to show the extents of its deviations from thermodynamic equilibrium due to different processes in a variety of environments, which the commonly used tracers such as $\delta^{13}C$ and $\delta^{18}O$ cannot provide. We also explore the potential of Δ_{47} in air CO_2 to identify/quantify the contribution from various sources. Atmospheric CO_2 over ocean is found to be in thermodynamic equilibrium with the surrounding surface sea water. Also respired CO_2 is in close thermodynamic equilibrium at ambient air temperature. In contrast, photosynthetic activity results in significant deviation in Δ_{47} values from that expected thermodynamically demonstrated using CO_2 collected from a controlled greenhouse. The disequilibrium could be a consequence of kinetic effects associated with the diffusion of CO_2 in and out of the leaf stomata. We also observe that $\delta^{18}O$ and Δ_{47} behave differently in response to photosynthesis unlike simple water-CO_2 exchange where the time scale of equilibration of the two is similar. Additionally, the measured Δ_{47} values in car exhaust CO_2 are significantly lower than the atmospheric CO_2 but higher than that expected at the combustion temperature. In urban and sub-urban regions, the Δ_{47} values are found to be lower than the thermodynamic equilibrium values at the ambient temperature, suggesting contributions from local combustion emissions.

Keywords: clumped isotopes; atmospheric CO_2; thermodynamic equilibrium; anthropogenic; car exhaust

Biogeosciences Discuss., doi:10.5194/bg-2016-106, 2016
Manuscript under review for journal Biogeosciences
Published: 18 April 2016

1. Introduction

The budget of atmospheric CO_2 is widely studied using the temporal and spatial variations of the concentration and bulk isotopic compositions ($\delta^{13}C$ and $\delta^{18}O$) of CO_2 (Francey and Tans, 1987; Francey et al., 1995; Yakir and Wang, 1996; Ciais et al., 1995a,b, 1997; Peylin et al., 1999; Cuntz et al., 2003; Drake et al., 2011; Welp et al., 2011; Affek and Yakir., 2014). $\delta^{13}C$ is useful to differentiate the exchange of CO_2 with the ocean and land biospheres as the photosynthetic discrimination against ^{13}C during exchange with land plants is higher than that associated with the chemical dissolution of CO_2 in the ocean (e.g., Tans et al., 1993; Ciais et al., 1995a; Francey et al., 1995; Ito, 2003; Bowling et al., 2014). $\delta^{18}O$ is used for partitioning global-scale net CO_2 terrestrial fluxes between photosynthesis and respiration (Francey and Tans, 1987; Farquhar and Lioyd, 1993; Yakir and Wang, 1996; Ciais et al., 1997; Peylin et al., 1999; Murayama et al., 2010; Welp et al., 2011). This is because oxygen isotopes in CO_2 exchanges readily with water and hence the values of $\delta^{18}O$ are different when exchanging with soil water or relatively enriched leaf water; the enrichment in ^{18}O in the leaf water occurs during evapotranspiration. The major limitation of $\delta^{13}C$ is that it cannot distinguish between CO_2 produced from high temperature combustion and low temperature respiration. $\delta^{18}O$ in atmospheric CO_2 is mainly controlled by various water reservoirs (ocean, leaf, and soil). In urban locations, a significant fraction of CO_2 may have combustion origin possessing $\delta^{18}O$ signature of atmospheric O_2 (Kroopnick and Craig, 1972; Ciais et al., 1997; Yakir and Wang, 1996; Barkan and Luz, 2012). The $\delta^{18}O$ values from these processes and interactions are different. As a result, $\delta^{18}O$ in atmospheric CO_2 has been widely used for constraining the budget of CO_2 (Francey and Tans, 1987; Ciais et al., 1997; Gillon and Yakir, 2001; Cuntz et al., 2003; Welp et al., 2011). However, due to its short turnover time in the atmosphere, mainly affected by presence of enzyme carbonic anhydrase in plants, soils, and surface ocean, the definite determination of the associated fluxes in CO_2 biogeochemical models remains inconclusive. The presence of diverse $\delta^{18}O$ reservoirs and processes such as evapotranspiration also complicates the interpretation.

The doubly substituted isotopologues or clumped isotopes such as $^{13}C^{18}O^{16}O$ in CO_2, whose excess over the stochastic isotopic distribution, denoted by Δ_{47}, provides an additional and independent constraint to study the atmospheric CO_2 budget and mechanisms for CO_2 production and consumption. Unlike bulk isotopes, clumped isotope studies for the atmospheric CO_2 are very limited mainly because of the challenges to acquire it precisely (Eiler and Schauble, 2004; Affek et al., 2007; Yeung et al., 2009). The available data are not sufficient to address some key issues such as quantification of CO_2 from different sources and to what extent the air CO_2 is in thermodynamic equilibrium with leaf and surface waters, especially in regions with strong anthropogenic activities such as urban areas. Also the effect of photosynthesis on the Δ_{47} of air CO_2 has not been studied rigorously. $\delta^{18}O$ and Δ_{47} were reported to have similar isotope exchange time scales with pure water (Affek, 2013; Clog et al., 2015), but how they behave in presence of other processes such as photosynthesis and respiration has not been studied well. A combined assessment from all of the three aforementioned isotopic tracers can better constrain the budget of CO_2 and associated processes than $\delta^{13}C$ or $\delta^{18}O$ alone.

Theoretically it is shown that in thermodynamic equilibrium, Δ_{47} values of CO_2 are temperature dependent (Eiler and Schauble, 2004; Wang et al., 2004), verified over a wide range from 10 to 1000 ^oC (Dennis et al., 2011). Processes that involve CO_2 and liquid water as medium, such as isotopic exchange with ocean water are expected to have Δ_{47} values close to the thermodynamic equilibrium. Δ_{47} values in ambient air CO_2 should reflect a balance of CO_2 fluxes between biosphere-atmosphere exchange, ocean-atmosphere exchange, and emissions from combustion sources. Photosynthesis involves gas phase diffusion of CO_2 into leaves, fixes ~1/3 of the CO_2, and returns the rest back to the atmosphere. CO_2 molecules inside a leaf are generally expected to be in thermodynamic equilibrium with leaf water because of presence of enzymatic carbonic anhydrase that greatly enhances the isotopic exchange (Cernusak et al., 2004). Δ_{47} values of soil respired CO_2 is also not well constrained, though it is believed to be in thermodynamic equilibrium with the soil water.

Here, we present clumped and bulk isotope data in near surface air CO_2 covering a wide variety of processes and interactions. Air samplings were made in South China Sea, two coastal stations in northern Taiwan, an urban traffic street, a sub-urban location, a forest site, a greenhouse, top of a high mountain, and car exhausts. The study is designed and aimed to show the extents of the deviations of near surface atmospheric CO_2 from thermodynamic equilibrium with local surface water. Possible influences from other processes such as anthropogenic emission, respiration, and photosynthesis on clumped isotopes are explored. We show that CO_2 respired from root and soil is in close thermodynamic equilibrium with the soil waters but photosynthesis tends to deviate it. Therefore, utilizing Δ_{47} for partitioning fluxes between photosynthesis and respiration/soil invasion is possible.

2. Materials and methods

Stable isotopic compositions of CO_2 including mass 47 amu were measured using a Finnigan MAT 253 gas source stable isotope ratio mass spectrometer configured to measure ion beams corresponding to M/Z 44 through 49. The instrument registers the major ion beams (44, 45 and 46) through resistors 10^8, 3×10^{10}, and 10^{11} Ohm, respectively, and minor ion beams (47, 48 and 49) through 10^{12} Ohm. All the measurements were carried out at Research Center for Environmental Changes, Academia Sinica, Taiwan.

Air samples were collected in 2L flasks and compressed to 2 atmosphere pressure using a membrane pump; the flasks were first flushed with the ambient air for ~10 min before sample collection. The air was pumped through a column packed with magnesium perchlorates to remove moisture. The moisture content was reduced from the ambient value of 70-90 % to less than 1 % relative humidity, checked using a LI-COR infrared gas analyzer (model 840A, LI-COR, USA).

To show how photosynthesis and respiration affect the abundances of CO_2 isotopologues and to demonstrate what different information the Δ_{47} can give from the other isotopologues, we performed systematic analyses for CO_2 collected in a controlled greenhouse with cemented floor located in the top (3^{rd}) floor of the Greenhouse Building, Academia Sinica. The size of the greenhouse was about 8m long, 5m wide and 5m high, and was in a condition to have minimal air exchange with the surroundings by switching off the ventilation system. More than 70 % of the ground area inside the greenhouse was occupied with *Cinnamomum cassia* plants, each of ~2 m height kept in pots. Samples were collected at intervals of less than half an hour to a few hours on three sunny days and one cloudy day to investigate the influence of photosynthesis and respiration on the isotopologues of CO_2. The greenhouse was isolated from the surroundings at least a day before the sample collection; the room relative humidity was ~50-70 % for the three sunny days and was above 90 % for the cloudy day.

Biogeosciences Discuss., doi:10.5194/bg-2016-106, 2016
Manuscript under review for journal Biogeosciences
Published: 18 April 2016

Forest air CO_2 was collected from a dense natural forest at the west end of the Academia Sinica Campus. The samples were collected ~100 m inside the forest on a small plateau at a height of ~30 m from the ground in the slope of a hill; the dense vegetation allowed little sunlight penetrating to the surface. The relative humidity at the site was 80-90 % during the sampling days and wind speed was nearly zero due to presence of hills on three sides of the sampling spot. Marine air was collected during a cruise in the South China Sea (for the cruise track see Figure 1) and from two coastal stations: Keelung (25°09′6″ N, 121°46′22″ E) and Fuguei Cape (25°18′ N, 121°32′ E) (Figure 1). Urban air was collected at a bus stop on Roosevelt Road, a busy street in Taipei. Sub-urban air was collected from an open roof (~30 m above ground) of Institute of Earth Science Building, Academia Sinica (AS; 25°2′41″ N, 121°36′52″ E); grassland air was collected from a grass field in front of the Department of Atmospheric Science, National Taiwan University Campus (NTU; 25° 1′ N, 121°30′ E), Taipei. In addition, we collected air from the summit of the Hehuan mountain (24°8′15″ N, 121°16′32″ E, 3.3 km a.s.l.) (Figure 1) on 9th October, 2013. All air samplings were made when there was no rain to avoid direct interaction with the rainwater. Car exhausts were collected from a Mazda 3000cc TRIBUTE and a Mitsubishi 2400cc New Outlander, using evacuated 2L glass flasks from ~20 cm inside the exhaust pipes through a column of magnesium perchlorate.

CO_2 was extracted from air by cryogenic technique. Air in the flask was pumped through a series of five coiled traps, with the first two immersed in dry ice-ethyl alcohol slush (-77 °C) for trace moisture removal followed by three in liquid nitrogen (-196 °C). CO_2 was collected from the traps immersed in liquid nitrogen by repeated freeze-thaw technique at liquid nitrogen and dry ice temperatures for further removal of traces of water [see *Mahata et al.*, 2012 for details]. The air was pumped for 40-45 minutes at a controlled rate of ~90 mL/min using a mass flow controller; the pressure on the post mass flow controller was ~10 mm of Hg. No measurable isotopic fractionation caused by mass flow controller at this flow rate was observed, checked using several aliquots of air from a high volume compressed air cylinder (~40 L at 2000 psi). For car exhaust, an aliquot of exhaust air was transferred to a 60 mL

Biogeosciences Discuss., doi:10.5194/bg-2016-106, 2016
Manuscript under review for journal Biogeosciences
Published: 18 April 2016

bottle and CO_2 was fully extracted cryogenically following the same protocol as discussed above (but with mass flow controller step skipped).

CO_2 was further purified from other condensable species like N_2O, CH_4, and hydrocarbons by means of gas chromatography (Agilent 6890N, with a 3.0 m × 0.3 cm stainless steel column packed with PorapakQ 80/100 mesh, supplied by Supelco Analytical, Bellefonte, PA, USA) with the column kept at -10 °C. High purity helium (>99.9999 % supplied by Air Products and Chemicals, Inc.) at 20 mL/min was used as carrier gas. CO_2 was eluted first, followed forthwith by N_2O, and CH_4, hydrocarbons and traces of water came out much later. To get an optimized condition for CO_2, we checked the separation of CO_2 from N_2O with varying proportions and at various temperatures (25 °C to -20 °C) and found a temperature of -10 °C at which column separated CO_2 from N_2O perfectly (see Supporting Information). The column was baked at 200 °C for more than 2 hours prior to use. The conditioned column is good for purifying three samples. At the end of the day, long baking (8-10 hours) was performed. At the initial phase the working gas was taken from a high purity commercial CO_2 called AS-2 ($\delta^{13}C$ = -32.54 ‰ and $\delta^{18}O$ = 36.61 ‰) procured from a local supplier (Air Products and Chemicals, Inc.). As the difference between the isotopic compositions of samples and AS-2 was high, we later changed the reference to Oztech CO_2 ($\delta^{13}C$ = -3.59‰ and $\delta^{18}O$ = 24.96 ‰) (Oztech Trading Corporation, USA) from December 2014 onward. No detectable difference in isotopic compositions including Δ_{47} was observed between the analyses from different working references. All $\delta^{13}C$ values are expressed in VPDB scale and $\delta^{18}O$ in VSMOW scale, unless specified otherwise. Δ_{47} is calculated following (Affek and Eiler, 2006):

$$\Delta_{47}=\left[\frac{R^{47}}{2R^{13}R^{18}+2R^{17}R^{18}+R^{13}\left(R^{17}\right)^2}-\frac{R^{46}}{2R^{18}+2R^{13}R^{17}+\left(R^{17}\right)^2}-\frac{R^{45}}{R^{13}+2R^{17}}+1\right]\times 1000 \quad (1)$$

where R^{13} and R^{18} (ratios $^{13}C/^{12}C$ and $^{18}O/^{16}O$) are obtained by measuring the traditional masses 44, 45 and 46 in the same CO_2 sample and R^{17} is calculated assuming a mass dependent relation with R^{18} given by $R^{17}=R^{17}_{VSMOW}\left(R^{18}/R^{18}_{VSMOW}\right)^{\lambda}$, where exponent λ=0.5164 is used for all Δ_{47} calculations (Affek and Eiler, 2006). The value of λ varies between 0.516 and 0.523 (Hoag et al., 2005; Barkan and Luz, 2012; Hoffmann et al., 2012; Thiemens et al., 2014). The variation in Δ_{47} is less than 0.01 ‰ at 25 °C when the exponent is varied over the aforementioned range. This variation is comparable to the measurement uncertainty and hence is not considered here; all the calculations are based on λ=0.5164. Δ_{47} is obtained by measuring CO_2 with respect to which the isotopes among various CO_2 isotopologues are distributed randomly (Δ_{47} ~ 0 ‰). Practically, this limit is approached by heating CO_2 at 1000 °C for more than two hours (Eiler and Schauble, 2004; Affek and Eiler, 2006). Measurements were made with a stable ~12 volt signal at mass 44, with peak centring, background scanning, and pressure-balancing before each acquisition started. Each sample was analyzed for 10 acquisitions, 10 cycles each at an integration time of 8 s; the total analysis time was approximately 2.5 h. Routine analysis of masses 48 and 49, in addition to masses 44 to 47 was used to monitor the degree of possible interference of sample impurities on the measurements of Δ_{47} (Ghosh et al., 2006).

Dependence of Δ_{47} on δ^{47} was derived by artificially varying the δ^{47} value by ~130 ‰ (Figure S1 in Supporting Information). δ^{47} is approximately equal to the sum of $\delta^{13}C$ and $\delta^{18}O$ measured with respect to the working gas. The wide range in δ^{47} was obtained by equilibrating AS-2 CO_2 with different waters covering a wide range of $\delta^{18}O$ (-106 to +22 ‰) at two temperatures (17 and 32 °C). CO_2 was separated from water-CO_2 mixture cryogenically and purified using gas chromatography as mentioned earlier. The extracted CO_2 was divided into two aliquots: one was directly analyzed in the mass spectrometer and the other was measured after heating at 1000 °C (to define scrambled/stochastic distribution) for more than two hours. A weak dependence of Δ_{47} on δ^{47} with a slope of -0.0017‰/‰ (Δ_{47}/δ^{47}) was observed. No pressure baseline correction was made considering the little dependence of Δ_{47} on δ^{47} (He et al., 2012). The calibration curve was then applied evenly to all samples to remove the dependence of Δ_{47} on δ^{47} (Ghosh et al., 2006; Huntington et al., 2009; Dennis et al., 2011). Details are provided in the Supporting Information.

The reference frame equation or empirical transfer function can then be derived from these three temperature experiments. All the Δ_{47} values are expressed in absolute reference frame (ARF) (Dennis et al., 2011). The empirical transfer function for the present case is $\Delta_{47-RF} = 1.0996\,\Delta_{47-[EGvsWG]o} + 0.9145$ with R^2= 0.9999 (n=3), where $\Delta_{47\text{-}RF}$ is the Δ_{47} value in the ARF and $\Delta_{47\text{-}[EGvsWG]o}$ is the intercept of the Δ_{47} versus δ^{47} plot. To obtain the temperature from the Δ_{47} values, we used the following relation (Dennis et al., 2011):

Biogeosciences Discuss., doi:10.5194/bg-2016-106, 2016
Manuscript under review for journal Biogeosciences
Published: 18 April 2016

$$\Delta_{47} = 0.003\left(\frac{1000}{T}\right)^4 - 0.0438\left(\frac{1000}{T}\right)^3 + 0.2553\left(\frac{1000}{T}\right)^2 - 0.2195\left(\frac{1000}{T}\right) + 0.0616 \quad (2)$$

The reproducibility (1-σ standard deviation) for air CO_2 measurements was established from three aliquots of CO_2 extracted from a compressed air cylinder with CO_2 concentration ($[CO_2]$) of ~388 ppmv. The 1-σ standard deviations were 0.07, 0.08, and 0.01 ‰ for $\delta^{13}C$, $\delta^{18}O$, and Δ_{47}, respectively (Table S1). We also used IAEA NBS-19 carbonate standard to check the reproducibility of our measurements routinely. For carbonate analysis, CO_2 was produced by reacting with ~104 % orthophosphoric acid at 25 °C. The measured isotopic data including Δ_{47} for NBS-19 are presented in Table 1, and the long term reproducibility is 0.014 ‰ (1-σ standard deviation; n=15). The accuracy from the measurements of NBS-19 is difficult to check, due to poor consensus of the reported Δ_{47} values from different laboratories; our values fall within the range. To further verify the accuracy, we equilibrated cylinder CO_2 (AS-2) with water at 15±2 °C and 25±2 °C, chosen to represent the ambient temperatures presented in the current study. The deviation of temperature from the expected values obtained from Δ_{47} was found to vary between -1 to +3 °C (Table S2).

For $[CO_2]$ measurements, flasks of volume 350 cc were used. These small flasks were connected in series with the larger flasks used for isotopic measurements. $[CO_2]$ was measured using a LI-COR infrared gas analyzer (model 840A, LI-COR, USA) at 4 Hz, smoothed with 20-s moving average. The analyzer was calibrated against a working standard (air compressed in a cylinder) with a nominal $[CO_2]$ of 387.7 ppmv and a CO_2 free N_2 cylinder. The reproducibility of LI-COR is better than 1 ppmv. The working standard was calibrated using a commercial Picarro analyzer (model G1301, Picarro, USA) by a series of NOAA/GMD certified tertiary standards with $[CO_2]$ of 369.9, 392.0, 409.2, and 516.3 ppmv, with a precision (1-σ standard deviation) of 0.2 ppmv. The $[CO_2]$ in car exhausts were estimated by gravimetric technique using an MKS Baratron gauge.

Ambient temperatures were taken from the nearest governmental weather stations (operated by Central Weather Bureau, Taiwan): Nankang (for AS; station code: C0A9G0; 25°03′27″ N, 121°35′41″ E, 42 m a.s.l.), Taipei (for NTU; station code: C1A730; 25°00' 58″ N, 121°31' 53″ E; 22 m a.s.l.), Hehuan mountain (station code: C0H9C1; 24°08′41″ N, 121°15′

Biogeosciences Discuss., doi:10.5194/bg-2016-106, 2016
Manuscript under review for journal Biogeosciences
Published: 18 April 2016

51″ E, 3240 m a.s.l.), and Keelung coast (for the two coastal sites; station code: 466940; 25°08′05″ N, 121°43′56″ E, 26.7 m a.s.l.).

3. Results

3.1 Greenhouse CO_2

Intraday variation in the concentration and isotopic compositions of CO_2 inside the controlled greenhouse is shown in Figure 2. The lowest [CO_2] and highest $\delta^{13}C$ and $\delta^{18}O$ values are observed during late morning hours while highest [CO_2] and lowest $\delta^{13}C$ and $\delta^{18}O$ values are observed during night time and early morning before sunrise (Table 2 and Figure 2A-2C), indicating that respiration and photosynthesis play the major role in controlling the variations of the [CO_2] and isotopic compositions. Keeling graphical analysis for $\delta^{13}C$ gives an intercept of -26.32±0.40 ‰ (Figure 2D), a value expected for C_3 plant respired CO_2. The Keeling plot for $\delta^{18}O$ gives an intercept of 30.68±0.73 ‰ (Figure 2E), which could be explained by a combined effect of respired CO_2 equilibrated with soil water and kinetic fractionation associated with the diffusion of CO_2 from soil to the air. The tight correlations among [CO_2], $\delta^{13}C$ and $\delta^{18}O$ (Figure 2D-2F), however, suggest that photosynthesis/respiration are the dominant processes controlling their variations and the mixing with ambient air and anthropogenic contribution of CO_2 are insignificant.

In contrast, Δ_{47} shows different patterns of diurnal variability. Figures 3A-3D detail diurnal variations in Δ_{47} in the greenhouse CO_2 in four different days. The first three are bright sunny days while the last one is a dark cloudy day; to further reduce photosynthetic activity, two layers of black cloths that cut down incident sunlight by ~50% are deployed for the last. The measured Δ_{47} values are also compared with the thermodynamic equilibrium. The maximum value of Δ_{47} is observed in the morning before ~8 AM and at night: the values are similar to that expected at the ambient temperatures, indicating that the respired CO_2 is in close thermodynamic equilibrium. The daytime Δ_{47} values are, in general, higher than the thermodynamic equilibrium values. By comparing the Δ_{47} values acquired in the sunny days with that in the cloudy day, we notice that when photosynthesis is weak, the Δ_{47} value is close to the thermodynamic equilibrium (Figure 4). No correlation ($R^2 < 0.1$) is observed between Δ_{47} and [CO_2], $\delta^{13}C$ or $\delta^{18}O$ (Figure 3A-C) except when the photosynthesis is weak (Figure

Biogeosciences Discuss., doi:10.5194/bg-2016-106, 2016
Manuscript under review for journal Biogeosciences
Published: 18 April 2016

3D), which suggests that the Δ_{47} carries information different from concentration and bulk isotopes when photosynthesis occurs. See Section 4.1 for detailed discussion.

3.2 Car exhaust

The concentration, $\delta^{13}C$ and $\delta^{18}O$ values of car exhaust CO_2 are 39350±50 ppmv, -27.70±0.03 ‰ and 25.35±0.07 ‰, respectively (Table 3). $\delta^{13}C$ value is similar to that reported elsewhere (Newman et al., 2008; Popa et al., 2014), the $\delta^{18}O$ is slightly higher than the atmospheric O_2 (~23.5 ‰), the source of O_2 for combustion. This is probably due to post isotopic exchange with water present in the stream of the exhaust inside the catalytic converter and the exhaust pipe. The average value of Δ_{47} for the exhausts from the two cars is 0.273±0.021 ‰, which gives an average temperature of 282±17 °C (Table 3).

3.3 CO_2 over ocean, coasts and land

Isotopic compositions including Δ_{47} values obtained for CO_2 over ocean, coasts, sub-urban, and grassland are summarized in Table 4 and 5. The averaged [CO_2] over ocean between latitudes 18°03′ N and 21°17′ N is 395±7 ppmv, and the values of $\delta^{13}C$ and $\delta^{18}O$ are -8.43±0.19 ‰ and 40.72±0.20 ‰, respectively (Table 4). Figure 5 shows a comparison of carbon Keeling analyses for the atmospheric CO_2 collected over different regions. The intercept for oceanic CO_2 is -15.96±1.95 ‰ (Figure 5A). In the coastal stations, the averaged values of [CO_2], $\delta^{13}C$, and $\delta^{18}O$ are 397±10 ppmv, -8.48±0.11 ‰, and 40.70±0.29 ‰, respectively, with a $\delta^{13}C$ Keeling intercept of -12.20±1.11 ‰ (Figure 5B). Both the [CO_2] and $\delta^{13}C$ values over the ocean and coasts are similar to those observed at Mauna Loa during the sampling period, suggesting little contribution from local/regional anthropogenic sources. However, the intercepts of the Keeling plots is different from the $\delta^{13}C$ value of the CO_2 released by the remineralization of organic matter (-20 to -30 ‰) in the deep sea regions, the expected source of CO_2 over ocean. This is probably due to partial isotopic equilibration of the CO_2 with dissolved inorganic carbon before releasing to the atmosphere (see discussion for details).

Biogeosciences Discuss., doi:10.5194/bg-2016-106, 2016
Manuscript under review for journal Biogeosciences
Published: 18 April 2016

The averaged values of [CO_2], $\delta^{13}C$, and $\delta^{18}O$ for air CO_2 near Roosevelt Road, a busy street in downtown Taipei, are 500±50 ppmv, -11.05±0.90 ‰, and 39.319±0.94 ‰, respectively (Table 5). Both the [CO_2] and isotopic compositions show signatures of a significant contribution from vehicular emissions. In the sub-urban location (AS), [CO_2] averaged over four months is 410±10 ppmv (Table 5), ~15 ppmv higher than that observed over the South China Sea and that at Mauna Loa Observatory during the time of sampling. The higher [CO_2] suggests contribution from local anthropogenic emissions. $\delta^{13}C$ values mainly vary between -7.83 to -10.30 ‰, with an average of -8.78±0.50 ‰. Keeling analysis for $\delta^{13}C$ (Figure 5C) gives an intercept of -26.16±1.58 ‰, indicating source of CO_2 from C_3 plant respiration and/or combustion. The averaged [CO_2] over the grassland (NTU) is 410±33 ppmv. The Keeling plot intercept is -16.98±1.02 ‰ (Figure 5D), indicating a significant fraction of CO_2 originated from C_4 vegetation. This is not surprising as the CO_2 was sampled over a C_4 dominated grassland (area: ~50 m x 50 m). We note that though the station is located in an urban region, the sampling location is at least ~150 m away from traffic streets, such as Keelung road, along with ~60 m wide, ~10 m high C_3 trees in between. As a result, anthropogenic signals are not very prominent. The averaged values of $\delta^{13}C$ and $\delta^{18}O$ are -8.95±0.70 ‰ and 39.74±1.00 ‰, respectively. Unlike greenhouse CO_2, no statistically significant correlation between $\delta^{18}O$ and 1/[CO_2] in air CO_2 in these sites is observed (not shown), probably due to various contributions from multiple sources and processes affecting CO_2.

The [CO_2], $\delta^{13}C$, and $\delta^{18}O$ values for two high mountain air CO_2 samples collected on 9th October, 2013 are 364 ppmv, -8.23±0.02 ‰ and 40.59±0.30 ‰, respectively (Table 5). The lower [CO_2] and higher $\delta^{13}C$ than Mauna Loa suggests photosynthetic uptake, which is also seen at NTU site and inside greenhouse on a few occasions. The air [CO_2], $\delta^{13}C$ and $\delta^{18}O$ are 438±16 ppmv, -9.99±0.50 ‰ and 40.39±0.63 ‰, respectively, for a dense forest site near the Academia Sinica (AS) Campus. Given the proximity of the site from AS, the higher concentration and lower $\delta^{13}C$ values than those at AS indicate significant influence from local respiration (Table 5).

Figure 6 shows the time series of $\delta^{13}C$ and $\delta^{18}O$ at the sub-urban station where measurements were carried out for more than four months. Tentatively, [CO_2] level increases and $\delta^{13}C$ depletes from October to February (Figure 6A), likely a result of seasonal variation in photosynthesis/respiration. On average, the $\delta^{13}C$ value is slightly less than the global mean,

Biogeosciences Discuss., doi:10.5194/bg-2016-106, 2016
Manuscript under review for journal Biogeosciences
Published: 18 April 2016

implying influence from local/regional anthropogenic activities though the dominant role is played by biogeochemistry in affecting the variation. The time series of $\delta^{18}O$ (Figure 6B) shows variation between 39.40 and 41.57 ‰, with an average of 40.87±0.46 ‰. An increasing trend is also observed in $\delta^{18}O$ from October to February. We attribute this to interactions with rain and surface waters which are heavier in winter time compared to the summer (Peng et al., 2010; Laskar et al., 2014).

The Δ_{47} values vary between 0.880 ‰ to 0.946 ‰ for the marine and coastal CO_2 (Table 4, Figures 7A and 7B), similar to that predicted at thermodynamic equilibrium at sea surface temperatures (obtained using equation (2)). Similarly, $\delta^{18}O$ of air CO_2 shows the expected equilibrium values with the surface sea water (see discussion), suggesting that the air CO_2 is indeed in thermodynamic equilibrium with the underlying sea water. Figure 7C shows the measured Δ_{47} values at the sub-urban station along with the equilibrium values expected at the ambient temperatures. Here the Δ_{47} values vary between 0.853 ‰ and 0.972 ‰, which in contrast to the marine CO_2, are significantly less than the thermodynamic equilibrium values (assuming water bodies have the same temperature as the ambient) (Table 5). Figure 7D shows the Δ_{47} values in the grassland (NTU). A large variation in Δ_{47} is observed (0.885 - 0.989 ‰) with an average of 0.937±0.030 ‰; some of the values are close to the thermodynamic equilibrium while the others deviated significantly. The forest air CO_2 Δ_{47} values in summer fall in the range of 0.887 ‰ to 0.920 ‰, with an average of 0.895±0.012 ‰ (Table 5). The values are similar to that at thermodynamic equilibrium (Figure 7E) except on 11th August, when a significant increase in Δ_{47} was observed. The deviation is probably due to influence of a super typhoon, which passed over the region on previous days mixing and transporting air masses regionally. In the high mountain station, the averaged value of Δ_{47} is 0.904±0.009 ‰, slightly less than that expected at the ambient temperature (Table 5).

To show how anthropogenic emission affects the background Δ_{47} values, we collected several air CO_2 samples from Roosevelt Road and the values are in the range of 0.754‰ to 0.833 ‰, with an average of 0.807±0.028 ‰ (Figure 7F). The value is lower by ~0.16 ‰ compared to the thermodynamic equilibrium value, indicating a significant fraction of CO_2 produced at higher temperatures.

4. Discussion

As stated earlier, the Δ_{47} has the unique physical property of representing the formation temperature of a CO_2 molecule, providing an alternative tool for constraining the budget of CO_2 in the atmosphere. We present in detail the data of multiple CO_2 isotopologues obtained from a controlled greenhouse, where atmospheric mixing and transport are largely reduced, to demonstrate the advantage of utilizing Δ_{47} for flux partitioning between photosynthesis and respiration over other CO_2 isotopologues. The data collected from other natural environments are also presented, compared, and discussed.

In urban and industrial places where anthropogenic emission is significant, all the three isotopic tracers, viz., $\delta^{13}C$, $\delta^{18}O$, and Δ_{47}, provide information about the anthropogenic fraction of CO_2 due to distinct values of their sources. For example in a traffic street, a two end member (background and anthropogenic CO_2) mixing of any of these tracers may provide sufficiently good estimate of the anthropogenic fraction of CO_2. However, if a significant fraction of CO_2 is respired from soil under C_3 plants, $\delta^{13}C$ cannot distinguish between the respired and anthropogenic sources. $\delta^{18}O$ is always not applicable due to complexity of multiple oxygen-containing sources. Anthropogenic CO_2 can also be quantified using radiocarbon (^{14}C) as fossil fuels are highly depleted in ^{14}C (Miller et al., 2012); however, it cannot distinguish difference between CO_2 from two sources with modern carbon.

The un-catalyzed isotopic exchange time scale between CO_2 and water is similar for both $\delta^{18}O$ and Δ_{47} (e.g., see Affek, 2013), and therefore, we expect that the two provide similar information when CO_2 in air simply exchanges with water. But it is not well understood if they behave similarly when biogeochemical processes such as photosynthesis and respiration are involved. We note that ^{18}O is highly variable between reservoirs such as leaf water affected by evapotranspiration even when temperature variation is not very large. Thus, Δ_{47} can complement $\delta^{18}O$ and ^{14}C data to probe the associated processes in the CO_2 cycling. A detailed analysis of the results from different locations is presented below.

4.1 Greenhouse CO_2

To minimize anthropogenic alteration and air mixing/transport and to maximize the variations of CO_2 isotopologues by biogeochemical processes, a controlled greenhouse

Biogeosciences Discuss., doi:10.5194/bg-2016-106, 2016
Manuscript under review for journal Biogeosciences
Published: 18 April 2016

provides an ideal environment. Diurnal variation is observed in [CO_2], $\delta^{13}C$, $\delta^{18}O$ (Figure 2), and Δ_{47} (Figure 3) in the greenhouse. Good correlations between [CO_2], $\delta^{13}C$ and $\delta^{18}O$ suggest common processes affecting all of them, and we believe they are photosynthesis and respiration. Giving July 31st as an example, we estimate the rates of night-time respiration and daytime photosynthetic uptake using the bulk isotopic compositions (Δ_{47} which will be discussed separately). The dimension of the greenhouse room is 8m, 5m and 5m (length, width and height). The night-time respiration rate is then estimated to be about ~10 ppmv per hour (considering change of [CO_2] from 5:30 PM to 9:30 PM; Figure 2A), or ~4×10^{13} molecules cm^{-2} s^{-1}. The increase of [CO_2] can be satisfactorily explained assuming C_3 respiration as the main source of CO_2 ($\delta^{13}C$ ≈ -26 ‰; intercept in Figure 2D) added to the background (-8.5 ‰). Similarly, the same conclusion is also arrived by analyzing $\delta^{18}O$ (the respired CO_2 is 30.68 ‰, intercept in Figure 2E, and background, $\delta^{18}O$ of air CO_2 outside, is 40 ‰). Thus, we conclude that the main factor that affects the changes in concentration as well as the isotopic compositions in night-time is respiration.

The daytime net uptake rate can be estimated by taking the changes from early morning to noon time; the [CO_2] reduces by 110 ppmv, $\delta^{13}C$ increases by 3.46 ‰, and $\delta^{18}O$ by 2.23 ‰ in about six hours. The estimated net photosynthetic uptake is ~7×10^{13} molecules cm^{-2} s^{-1}. Neglecting respiration during daytime, the photosynthetic discrimination can be calculated using the Rayleigh distillation model

$$R = R_o f^{\alpha-1} \tag{3}$$

where R_o and R are the initial and photosynthesis modified $^{13}C/^{12}C$ or $^{18}O/^{16}O$ ratios, respectively, f is the fraction of the material left, and α is the fractionation factor. The estimated discrimination in ^{13}C defined by (α-1), following equation (3), is -15.3 ‰, similar to that expected for C_3 type vegetation. For ^{18}O, in addition to photosynthetic uptake, one has to consider an additional effect due to temperature-dependent water-CO_2 equilibrium fractionation. That is, the process decreases $\delta^{18}O$ by ~0.2 ‰ for an increase of 1 ^oC in temperature (Brenninkmeijer et al., 1983); from morning to noon time, the temperature effect reduces $\delta^{18}O$ by -4.4 ‰. Adding this factor to the observed change in $\delta^{18}O$ yields a discrimination of about -27 ‰; the value becomes -9.5 ‰, if this additional temperature-dependence is ignored. The obtained discrimination factors for ^{13}C and ^{18}O are in good agreement with those reported previously (Farquhar et al., 1989; Flanagan et al., 1997; Cuntz et al., 2003; Affek and Yakir, 2014).

Assuming ca. 1/3 of the CO_2 molecules in stomata are fixed photosynthetically, the remaining retro-diffuse back to the atmosphere (Farquhar and Lloid, 1993), implying that the CO_2-water isotopic exchange rate is ~2×10^{14} molecules cm^{-2} s^{-1}, or 9 hours of oxygen isotope exchange time for CO_2 in the room. As a result, we do not expect that CO_2 reaches complete isotopic equilibrium with the substrate water in a few hours. Δ_{47} values in the leftover CO_2 can be used to check the disequilibrium. The respired CO_2 are found to be always in thermodynamic equilibrium at the ambient temperature, shown by the Δ_{47} values of CO_2 in the early morning and night-time (Figure 3A-3C) and that collected on a cloudy day with suppressed photosynthetic activity (Figure 3D). The close-thermodynamic equilibrium at reduced photosynthetic condition is also shown in Figure 4A that deviation from the expected is small. On sunny days, the [CO_2], $\delta^{13}C$, and $\delta^{18}O$ values change by 50-115 ppm, 2-4 ‰, and 1.1-2.2 ‰, respectively, in a time period of ~5 hours in the morning (Figure 2). Figure 3 shows that the Δ_{47} values retain the thermodynamic equilibrium values in the morning hours (until 9 AM) and deviate later on. The reduction and deviation in the Δ_{47} values during the time period is ~0.05 ‰ (Figures 3A-3C); the changes we believe are significant, as the values are much higher than the uncertainty of the measurements. We attribute this deviation to photosynthesis as it is seen when photosynthesis is strong. Strong influence of photosynthesis on Δ_{47} was also reported previously (Eiler and Schauble, 2004). Photosynthesis as a source of disequilibrium was further shown recently by analyzing the clumped isotopes of O_2 (Yeung et al., 2005). Though enzymatic carbonic anhydrase catalyzes the water-CO_2 isotopic exchange toward equilibrium (Peltier et al., 1995; Cernusak et al., 2004), the reaction may not complete, limited by the enzymatic activity inside leaves; large variation in the activity of carbonic anhydrase in different vegetation types (C_3, C_4) or within the same type is observed (see Gillon and Yakir, 2001 and references therein). Furthermore, a box modeling by Eiler and Schauble (2004) demonstrated that gas diffusion through leaf stomata during photosynthesis fractionates the remaining air CO_2 Δ_{47} values from the thermodynamic equilibrium set by leaf water. Mixing of more than one component can also cause change in Δ_{47} when bulk isotopic compositions of the components are different (Affek and Eiler, 2006), but this can easily be ruled out as it is not observed when photosynthesis is not very strong (Figure 3D). More rigorous investigations with controlled experiments using different plants with diverse carbonic anhydrase activities are needed to resolve the issue. We note that no significant correlation between $\delta^{18}O$ and Δ_{47} is observed (Figure 3). Therefore, the plant photosynthesis decouples Δ_{47} and $\delta^{18}O$; in contrast, pure water-CO_2 isotopic exchange process shows that the two behave similarly as far as isotopic equilibration is concerned (Affek, 2013; Clog et al. 2015).

The Δ_{47} thus serves as an independent tracer for studying photosynthesis. Though the deviation from equilibrium during photosynthesis is also observed in oxygen clumped isotopes [*Yeung et al*., 2015], CO_2 and O_2 are affected and produced from different processes and sources; the former is affected seriously by water (water-CO_2 isotopic exchange) while the latter is derived from water. We believe the analyses of the clumped isotopes for both CO_2 and O_2 are of great importance in the atmospheric carbon cycling study, providing a new angle for tackling the chemistry chain in photosynthesis. More systematic study in controlled environments including leaf level experiments will help to better understand the role of photosynthesis on Δ_{47}.

4.2 Marine and coastal air CO_2

The concentration and $\delta^{13}C$ values of marine air CO_2 are close to the background atmospheric values reported at Mauna Loa, indicating little contribution from local/regional anthropogenic activities. The Keeling analysis for $\delta^{13}C$ gives an intercept of -15.9±2.0 ‰ (Figure 5A) which is the $\delta^{13}C$ value of the source CO_2 over the ocean. The CO_2 released over ocean is mainly originated from the remineralization of organic matter in the deeper ocean, the $\delta^{13}C$ value of which ranges between -20 and -30 ‰ in the tropical to subtropical oceans (Francois et al., 1993; Goericke and Fry, 1994), the intercept observed here is much higher than this range. A possibility is that the remineralized CO_2 gets equilibrated with the dissolved inorganic carbon before releasing. Again a complete equilibration of the CO_2 with the dissolved inorganic carbon would lead to a $\delta^{13}C$ value of released CO_2 to be -9 to -10 ‰ (Mook, 1986; Boutton, 1991; Zhang et al., 1995; Affek and Yakir, 2014), the observed value of the intercept is much less than this. Therefore, we conclude that the CO_2 produced in the deeper ocean is partially equilibrated with the dissolved inorganic carbon before releasing to the atmosphere.

Biogeosciences Discuss., doi:10.5194/bg-2016-106, 2016
Manuscript under review for journal Biogeosciences
Published: 18 April 2016

The $\delta^{18}O$ values of the surface sea water in the region in summer (July-September) and winter (December-February) are about -1.7 ‰ and -0.6 ‰ (Ye et al., 2014). The sea surface temperatures in the summer and winter are about 28 and 24 °C, and the equilibrated $\delta^{18}O$ values of the atmospheric CO_2 should be 38.9 ‰ and 40.7 ‰, respectively (Brenninkmeijer et al., 1983). Our observed values lie in the range of 40.4 ‰ to 41.0 ‰ (Table 4), consistent with the isotopic equilibrium values with the surface water. Therefore, we conclude that oxygen isotopes in near surface air CO_2 over ocean are close to the isotopic equilibrium with the surface sea water. This conclusion is further supported by the observed Δ_{47} values. This is due to the same water-CO_2 exchange time for the two species (Affek, 2013; Clog et al., 2015). Comparing the greenhouse data above, we therefore conclude that $\delta^{18}O$ and Δ_{47} respond differently when photosynthesis is the main governing factor and behave similarly when exchange occurs due to simple water-CO_2 equilibration. Though carbonic anhydrase are also present in the surface ocean and marine phytoplankton does photosynthesis, $\delta^{18}O$ and Δ_{47} in air CO_2 over the ocean show the values at thermodynamic equilibrium unlike greenhouse. The degree of deviation from thermodynamic equilibrium likely increases with the strength of photosynthesis, and normally the oceanic photosynthesis is less compared to the terrestrial plants. Therefore, Δ_{47} can be used as a tracer for estimating terrestrial carbon uptake. Compared to $\delta^{18}O$, Δ_{47} is process sensitive and is not affected by the isotopic composition of substrate water. Given that the surface air temperature is better measured, we believe the clumped isotopes potentially provide good tracers for global carbon flux study involving CO_2, complementing the commonly used species like [CO_2], $\delta^{13}C$, and $\delta^{18}O$.

The isotopic values including Δ_{47} in the two coastal stations are similar to those observed for the marine CO_2. The carbon Keeling analysis yields an intercept of -12.20±1.11 ‰ (Figure 5D), consistent with that for the marine $\delta^{13}C$ (removing one outlier from Figure 5A gives an intercept of -13.3 ±1.0 ‰). The Δ_{47} values here are similar to the thermodynamic equilibrium with the sea surface water at the temperature of ~27 °C (Figure 7B). The recoded air temperature during the sampling period over the coasts varies between 14 and 24 °C and is not reflected in the Δ_{47} values. We note that the samples are collected from two open spaces in the coasts where strong north and northeasterly winds overwhelm, carrying air masses from the oceans towards the sampling locations (See Table S3 in Supporting Information). Therefore, we expect the major contribution is marine air with little influence from local

Biogeosciences Discuss., doi:10.5194/bg-2016-106, 2016
Manuscript under review for journal Biogeosciences
Published: 18 April 2016

processes, which could occasionally cause deviation from the thermodynamic equilibrium values.

4.3 Car exhaust CO_2

The Δ_{47} value of car exhaust CO_2 should reflect the temperature of fuel combustion inside the combustion chamber which is >800 ^oC. However, the temperature estimated from Δ_{47} is found to be 283±18 ^oC. It is likely that interaction of the sample CO_2 with the condensed water in the exhaust pipe modifies the Δ_{47} value: during sample collection, we observed that the exhaust gas contains a large amount of water vapor and some of which get condensed on the exhaust pipe and the front part of the magnesium perchlorate column. Precautions, such as opening the evacuated flask for a short time (<1 min) and careful holding of the sampling tube inside the exhaust pipe without touching the wall of the pipe, are taken to minimize CO_2-water interaction during sample collection.

The higher Δ_{47} value for the exhaust CO_2 indicates isotopic re-equilibration of CO_2 with water in the stream of the exhaust gas and inside catalytic converter, also supported by the observed enriched $\delta^{18}O$ than atmospheric O_2; the oxygen atoms in the two most abundant species, water and CO_2 here, are mostly originated from atmospheric O_2 and are expected to inherit the isotopic composition of atmospheric O_2. Normally isotopes in CO_2 do not exchange with water vapor, but inside catalytic converter, exchange may take place on the surface of the catalyst at certain temperature (which is usually much less than the combustion temperature). Affek and Eiler (2007) also observed elevated Δ_{47} values for car exhausts and estimated a temperature of CO_2 production to be ~200 ^oC. The temperature estimated here is significantly higher than that observed by Affek and Eiler (2007). Difference could be due to different car models and the variations in the temperatures of the catalytic converters from car to car.

4.4 Urban and sub-urban air CO_2

A significant fraction of anthropogenic CO_2 is present in the air CO_2 over the urban site, indicated by the $[CO_2]$ as well as isotopic compositions including Δ_{47}. Limits to the

Biogeosciences Discuss., doi:10.5194/bg-2016-106, 2016
Manuscript under review for journal Biogeosciences
Published: 18 April 2016

anthropogenic contribution can be estimated following a two component mixing: $\delta = f_{anth}\times\delta_{anth}+(1-f_{anth})\times\delta_{bgd}$, where δ's can be $\delta^{13}C$ or $\delta^{18}O$ or Δ_{47} and f's, the corresponding weighting factor, and subscripts 'anth' and 'bgd' refer to anthropogenic and background, respectively. We take the 'anthropogenic' and 'background' end member isotopic compositions from the car exhaust (Table 3) and marine CO_2 (Table 4), respectively. Assuming that the excess in [CO_2] above the background is originated from vehicular emissions, the values of the $\delta^{13}C$, $\delta^{18}O$, and Δ_{47} in the urban site obtained using the mixing equation are -12.26 ‰, 37.68 ‰, and 0.791 ‰, respectively, which are similar to those observed (Table 5). Δ_{47} is not a conserved quantity and a linear mixing is not valid when the bulk isotopic compositions of the components are widely different. In the present case, the isotopic compositions of the two components are not drastically different and fraction of anthropogenic CO_2 is much less (<1/4) than the background CO_2, and hence the error due to linear approximation is smaller than the uncertainty of measurement.

No systematic diurnal or temporal trend is observed in the Δ_{47} values in sub-urban CO_2 during the sampling period (Figure 7C) though a weak trend is seen in $\delta^{13}C$ and $\delta^{18}O$ (Figure 6), furthermore demonstrating that Δ_{47} behaves differently from [CO_2], $\delta^{13}C$, and $\delta^{18}O$. Almost all measured Δ_{47} values are lower than that expected at the ambient temperature except two days: 9th November, 2013 and 3rd February, 2014. $\delta^{13}C$ values are also slightly lower than the background values. The reduced values of Δ_{47} could be due to contribution of CO_2 from combustion processes which produce CO_2 with low Δ_{47} values as discussed in Section 4.3. We estimate the contribution of local anthropogenic emissions in $\delta^{13}C$ and Δ_{47} using the two components mixing discussed above. The components are the background air CO_2 and car exhausts. The expected $\delta^{13}C$ and Δ_{47} values of the mixture are -9.1 ‰ and 0.92 ‰, respectively. The observed Δ_{47} value is significantly different from that estimated from simple two component mixing, though it is not different for $\delta^{13}C$, suggesting other processes like photosynthesis present in affecting Δ_{47}. After subtracting the local anthropogenic contribution from the observed Δ_{47} values, a difference of ~0.026 ‰ between the observed and estimated remains for sub-urban station and it disappears for urban station (see Table S4 in Supporting Information). This is not obvious in $\delta^{13}C$ probably due to larger variation. The lower Δ_{47} values in sub-urban station could possibly be due to kinetic effect during photosynthetic assimilation, partial contribution of marine air, or a combination of them. The marine air in the vicinity of Taiwan, which is at thermodynamic equilibrium with the surface sea water as discussed earlier, may contribute partially to the air CO_2 at the sampling site. Varying contribution of marine air could explain the lower Δ_{47} values to some extent. The respired CO_2 is in thermodynamic equilibrium as shown above (Section 4.1). Therefore, the most plausible cause for observed deviation in the Δ_{47} values that cannot be accounted for by anthropogenic and marine alterations is photosynthesis, as discussed earlier for greenhouse CO_2. This is not unreasonable, as the Academia Sinica Campus is surrounded by thick greeneries.

On 9th Nov, 2013 and 3rd February, 2014, the Δ_{47} values are close to that expected at thermodynamic equilibrium (Figure 7C). The Δ_{47} values on 9th November are not very different from the values reported for the previous or next days. However, the calculated thermodynamic equilibrium values on that day are relatively low due to higher ambient temperatures (Figure 7C). On 3rd Febrauray, 2014, the Δ_{47} values are higher and comparable to the thermodynamic equilibrium values expected at ambient temperatures. A likely explanation is that on that day relatively strong wind from the southern land (Table S3 in Supporting Information) contributed the air CO_2 and higher Δ_{47} values are due to mixing of the local air with that transported from the south of Taipei.

4.5 Forest, grassland and high mountain air CO_2

An elevated CO_2 concentration and low $\delta^{13}C$ and $\delta^{18}O$ values indicate significant contribution of respiration and/or anthropogenic CO_2 in the forest station (Table 5) near the Academia Sinica Campus. Though the samples are collected at 10-11 AM under bright sunlight, the vegetation is so dense that little sunlight reached the ground. As a result, photosynthesis is weakened at the ground level. Also poor circulation of air due to presence of high heels on the three sides of the sampling spot makes the site nearly isolated from the surroundings. The Δ_{47} values are similar to the thermodynamic equilibrium expected at the ambient temperatures except on 11th August, 2015 on which a significantly higher Δ_{47} value is observed (Figure 7F). The higher value is likely due to the influence of the super Typhoon Soudelor which passed over Taipei during 8-10 August, 2015 causing a decrease in temperature by 3-4 ^{o}C and air masses mixing in a larger spatial scale.

In the grassland station in Taipei city, the Keeling plot for $\delta^{13}C$ gives an intercept of -17.0±1.0 ‰ (Figure 5D). This indicates some sources of CO_2 with higher $\delta^{13}C$ values compared to the most expected sources, namely, C_3 vegetation and vehicle emission with a $\delta^{13}C$ value of ~ -27 ‰. The samples are collected just above the surface of the grasses. Tropical warm grasses are mainly C_4 type with $\delta^{13}C$ in the range of -9 to -19 ‰ and a global average of -13 ‰ (Deines, 1980). We measured $\delta^{13}C$ values of a few grass samples and found values in the range of -15 to -17 ‰. The soil and grass respired CO_2 with higher $\delta^{13}C$ contributed significantly to the near surface CO_2, resulting in an elevated intercept of -17 ‰. The concentration is sometimes observed to be less than the background level, probably due to strong CO_2 uptake by plants. The temperature gradually decreased from 26 to 20 ^{o}C during the consecutive three days and clumped isotope followed similar trend, reflecting the influence of temperature on CO_2 Δ_{47} and rapid equilibration with the leaf and surface waters. The low value observed on the second day is probably due to plumes of vehicle exhausts, supported by the elevated level in [CO_2] and depletion in $\delta^{13}C$ and $\delta^{18}O$ (Table 5).

For high mountain CO_2, the Δ_{47} value (Table 5) is lower than that expected at ~10 ^{o}C, the ambient temperature at the top of the mountain site during sampling. The Δ_{47} values are similar to that observed in the plain and over the ocean. We note that during the sampling period, the site was affected significantly by winter monsoons. HYSPLIT 24 hours back trajectory shows marine origin of air (not shown) during the sampling time. The air CO_2 on the mountain probably does not get sufficient time to isotopically equilibrate with the local surface and leaf water but show the signature of the marine CO_2.

The deviations in Δ_{47} from the thermodynamic equilibrium values in different atmospheric environments and processes are summarized in Figure 8. It is obvious that the urban and sub-urban CO_2 deviate the most towards lower Δ_{47} values, mainly contributed by CO_2 originated from high temperature combustions, i.e., vehicular emissions. The respired CO_2 are always in close thermodynamic equilibrium at the ambient temperature. On the other hand, CO_2 affected by strong photosynthesis show significant deviation from the thermodynamic equilibrium values. Kinetic isotopic fractionation during diffusion of CO_2 in and out of leaf stomata is a probable reason.

5. Summary

Biogeosciences Discuss., doi:10.5194/bg-2016-106, 2016
Manuscript under review for journal Biogeosciences
Published: 18 April 2016

We presented a compilation of Δ_{47} analyses for car exhaust, greenhouse and air CO_2 over a wide variety of interactions in tropical and sub-tropical regions including marine, coastal, urban, sub-urban, forest, and high mountain environments. Car exhaust, urban, sub-urban and greenhouse air CO_2 significantly deviate from the thermodynamic equilibrium values. While respired CO_2 is in thermodynamic equilibrium with leaf and soil surface waters, photosynthesis significantly deviates the Δ_{47} values from the thermodynamic equilibrium. The Δ_{47} values in urban and sub-urban air CO_2 are lower than that expected under thermodynamic equilibrium at the ambient temperature. The deviation is mainly due to contributions from fossil fuel emissions and to some extent due to photosynthesis especially in regions with dense vegetation. We expect Δ_{47} can shed light on the estimation of anthropogenic contribution to the atmospheric CO_2 and the activity of photosynthesis. The latter deserves further investigation, to establish how exactly Δ_{47} is affected by photosynthesis, before the tracer can be used for estimating gross primary productivity.

Data availability

All the data used in the manuscript are also presented in the form of Tables.

Acknowledgement

We thank Dr. Chung-Ho Wang for providing waters with different $\delta^{18}O$, Institute of Earth Sciences, Academia Sinica for providing laboratory space, Mr. Frank Lin for helping sampling in greenhouse, Dr. Jia-Lin Wang and Dr. Chang-Feng Ou-Yang for calibrating compressed air cylinder, Mr. Hao-Wei Wei for collecting air at the campus of National Taiwan University and Mr. Wei-Kang Ho for collecting oceanic CO_2 and helping in laboratory setups. Special thanks to Prof. S. K. Bhattacharya and Dr. Sasadhar Mahata for helpful discussion. This work is supported by the Ministry of Science and Technology (MOST-Taiwan) grants 101-2628-M-001-001-MY4 and 103-2111-M-001-006 to Academia Sinica and Academia Sinica Career Development Award and MOST 103-2119-M-002-022 to National Taiwan University.

References

Affek H. P., and Eiler J. M.: Abundance of mass 47 CO_2 in urban air, car exhaust, and human breath, Geochim. Cosmochim. Acta, 70, 1–12, 2006.

Affek H. P., Xu X., and Eiler J. M.: Seasonal and diurnal variations of $^{13}C^{18}O^{16}O$ in air: Initial observations from Pasadena CA, Geochim. Cosmochim. Acta**,** 71, 5033–5043, 2007.

Affek H. P., and Yakir D.: The stable isotopic composition of atmospheric CO_2, Treaties of Geochemistry, 5, 179-212, 2014.

Affek, H. P.: Clumped isotopic equilibrium and the rate of isotope exchange between CO_2 and water, Am. J. Sci. 313 (4), 309–325, 2013.

Barkan E., and Luz B.: High precision measurements of $^{17}O/^{16}O$ and $^{18}O/^{16}O$ ratios in H_2O, Rapid Commun. Mass Spectrom., 19, 3737–3742, 2005.

Brenninkmeijer, C. A. M., Kraft, P and Mook, W. G.: Oxygen isotope fractionation between CO_2 and H_2O, Isot. Geosci., 1, 181-190, 1983.

Boutton, T. W.: Stable carbon isotope ratios of natural materials. II. Atmospheric, terrestrial, marine, and freshwater environments, in Carbon Isotope Techniques, edited by D. C. Coleman and B. Fry, pp. 173-185, Academic Press, New York, 1991.

Bowling, D. R., Ballantyne, A. P., Miller, J. B., Burns, S. P., Conway, T. J., Menzer, O., Stephens, B. B., and Vaughn, B. H.: Ecological processes dominate the ^{13}C land disequilibrium in a Rocky Mountain subalpine forest, Global Biogeochem. Cycles, 27, doi:10.1002/2013GB004686, 2014.

Cernusak, L. A., Farquhar, G. D., Wong, S. C., and Williams, H. S.: Measurement and Interpretation of the Oxygen Isotope Composition of Carbon Dioxide Respired by Leaves in the Dark, Plant Physiology, 136, 3350–3363, 2004.

Ciais, P., Denning, A. S., Tans, P. P., Berry, J. A., Randall, D. A., Collatz, G. J., Sellers, P. J., White, J. W. C., Trolier, M., Meijer, H. A. J., Francey, R. J., Monfray, P., and Heimann, M.: A three-dimensional synthesis study of $\delta^{18}O$ in atmospheric CO_2. 1. Surface fluxes, J. Geophys. Res. -Atm., 102, 5857–5872, 1997.

Ciais, P., Tans, P. P., Trolier, M., White, J. W. C., and Francey, R. J.: A large northern-hemisphere terrestrial CO_2 sink indicated by the $^{13}C/^{12}C$ ratio of atmospheric CO_2, Science, 269, 1098–1102, 1995a.

Ciais, P., Tans, P. P., White, J. W. C., Trolier, M., Francey, R. J., Berry, J. A., Randall, D. R., Sellers, P. J., Collatz, J. G., and Schimel, D. S.: Partitioning of ocean and land uptake of CO_2 as inferred by $\delta^{18}O$ measurements from the NOAA Climate Monitoring and Diagnostics Laboratory Global Air Sampling Network, J. Geophys. Res., 100, 5051–5070, 1995b.

Clog, M., Stolper, D., and Eiler, J. M.: Kinetics of CO2(g)–H2O(1) isotopic exchange, including mass 47 isotopologues, Chem. Geol., 395, 1-10, 2015.

Cuntz, M., Ciais, P., Hoffmann, G., Allison, C. E., Francey, R. J., Knorr, W., Tans, P. P., White, J. W. C., and Levin, I.: A comprehensive global three-dimensional model of $\delta^{18}O$ in atmospheric CO_2: 2. Mapping the atmospheric signal, J. Geophys. Res., 108, (D17), DOI: 10.1029/2002jd003153, 2003.

Deines, P.: The isotopic composition of reduced organic carbon, in: Handbook of Environmental Isotope Geochemistry, 1. The Terrestrial Environment, edited by Fritz, P. and Fontes, J. C. Elsevier, 329-406, 1980.

Dennis, K. J., Affek, H. P., Passey, B. H., Schrag, D. P., and Eiler, J. M.: Defining an absolute reference frame for 'clumped'isotope studies of CO_2, Geochim. Cosmochim. Acta, 75, 7117–7131, 2011.

Drake, J. E., et al.: Increases in the flux of carbon belowground stimulate nitrogen uptake and sustain the long-term enhancement of forest productivity under elevated CO_2, Ecology Letters, 14, 349–357, 2011.

Eiler, J. M. and Schauble, E.: $^{18}O^{13}C^{16}O$ in Earth's atmosphere, Geochim. Cosmochim. Acta, 68, 4767–4777, 2004.

Farquhar, G. D., Ehleringer, J. R., and Hubick, K. T.: Carbon isotope discrimination and photosynthesis, Annu. Rev. Plant. Physiol. Plant Mol. Biol., 40, 503-537, 1989.

Farquhar, G. D. and Lloyd, J.: Carbon and oxygen isotope effects in the exchange of carbon dioxide between plants and the atmosphere, in: Stable isotopes and plant carbon-water relations, edited by J. R. Ehleringer, A. E. Hall, and G. D. Farquhar, Academic Press, New York, 47–70, 1993.

Flanagan, L. B., Brooks, J. R., Varney, G. T., Ehleringer, J. R.: Discrimination against $C^{18}O^{16}O$ during photosynthesis and the oxygen isotope ratio of respired CO_2 in boreal forest ecosystems, Global Biogeochem. Cycles, 11(1), 83-98, 1997.

Francey, R. J. and Tans, P. P.: Latitudinal variation in O-18 of atmospheric CO_2, Nature, 327, 495–497, 1987.

Francey, R. J., Tans, P. P., Allison, C. E., Enting, I. G., White, J. W. C. and Trolier, M.: Changes in oceanic and terrestrial carbon uptake since 1982, Nature, 373 (6512), 326–330, 1995.

Francois, R., Altabet, M. A., Goericke, R., McCorckle, D. C., Brunet, C., and Poisson, A.: Changes in the $\delta^{13}C$ of surface water particulate organic matter across the subtropical convergence in the SW Indian Ocean, Global Biogeochem. Cycles, 7(3), 627-644, 1993.

Ghosh, P., Adkins, J., Affek, H. P., Balta, B., Guo, W., Schauble, E., Schrag, D., and Eiler, J. M.: ^{13}C–^{18}O bonds in carbonate minerals: a new kind of paleothermometer, Geochim. Cosmochim. Acta, 70, 1439–1456, 2006.

Gillon, J., Yakir, D.: Influence of carbonic anhydrase activity in terrestrial vegetation on the ^{18}O content of atmospheric CO_2, Science 291, 2584–2587, 2001.

Goericke, R. and Fry, B.: Variations of marine plankton $\delta^{13}C$ with latitude, temperature, and dissolved CO_2 in the world ocean, Global Biogeochem. Cycles, 8(1), 85-90, 1994.

He, B., Olack, G. A., and Colman, A. S.: Pressure baseline correction and high-precision CO_2 clumped isotope (Δ_{47}) measurements in bellows and micro-volume modes, Rapid Comm. Mass Spec., 26, 2837–2853, 2012.

Hoag, K. J., Still, C. J., Fung, I. Y., and Boering, K. A.: Triple oxygen isotope composition of tropospheric carbon dioxide as a tracer of terrestrial gross carbon fluxes, Geophys. Res. Lett., 32, L02802, doi:10.1029/2004GL021011, 2005.

Hofmann, M. E. G., Horváth, B., and Pack, A.: Triple oxygen isotope equilibrium fractionation between carbon dioxide and water, Earth Planet. Sci. Lett., 319–320, 159–164, 2012.

Huntington, K. W., Eiler, J. M., Affek, H. P., Guo, W., Bonifacie, M., Yeung, L. Y., Thiagranjan, N., Passey, B., Tripathi, A., Daëron, M., and Came, R.: Methods and limitations of 'clumped' CO2 isotope (Delta47) analysis by gas-source isotope ratio mass spectrometry, J. Mass Spectrom., 44(9), 1318-29. doi: 10.1002/jms.1614, 2009.

Ito, A.: A global-scale simulation of the CO_2 exchange between the atmosphere and the terrestrial biosphere with a mechanistic model including stable carbon isotopes, 1953–1999, Tellus 55B, 596–612, 2003.

Kroopnick, P., and Craig, H.: Atmospheric oxygen – Isotopic composition and solubility fraction, Science, 175, 54-55, 1972.

Landais, A., Barkan, E., Yakir, D., and Luz, B.: The triple isotopic composition of oxygen in leaf water, Geochim. Cosmochim. Acta, 70**,** 4105-4155, 2006.

Laskar, A. H., Huang, J. C., Hsu, S. C., Bhattacharya, S. K., Wang, C. H., and Liang, M. C.: Stable isotopic composition of near surface atmospheric water vapor and rain–vapor interaction in Taipei, Taiwan, J. Hydrol, 519, 2091-2100, 2014.

Mahata, S., Bhattacharya, S. K., Wang, C. H., and Liang, M. C.: An improved CeO_2 method for high-precision measurements of $^{17}O/^{16}O$ ratios for atmospheric carbon dioxide, Rapid Commun. Mass Spectrom., 26, 1909−1922, 2012.

Miller, J. B., Lehman, S. J., Montzka, S. A., et al.: Linking emissions of fossil fuel CO_2 and other anthropogenic trace gases using atmospheric $^{14}CO_2$, J. Geophys. Res., 117, D08302, doi:10.1029/2011JD017048, 2012.

Mook, W. G.: ^{13}C in atmospheric CO_2, Neth. J. Sea Res., 20, 211-23, 1986.

Murayama, S., Takamura, C., Yamamoto, S., Saigusa, N., Morimoto, S., Kondo, H., Nakazawa, T., Aoki, S., Usami, T., and Kondo, M.: Seasonal variations of atmospheric CO_2, $\delta^{13}C$, and $\delta^{18}O$ at a cool temperate deciduous forest in Japan: Influence of Asian monsoon, J. Geophys. Res., 115, D17304, doi:10.1029/2009JD013626, 2010.

Newman, S., Xu, X., Affek, H. P., Stolper, E., Epstein, S.: Changes in mixing ratio and isotopic composition of CO_2 in urban air from the Los Angeles basin, California, between 1972 and 2003, J. Geophys. Res., 113, D23304, doi:10.1029/2008JD009999, 2008.

Popa, M. E., Vollmer, M. K., Jordan, A., Brand, W. A., Pathirana, S. L., Rothe, M., Röckmann, T.: Vehicle emissions of greenhouse gases and related tracers from a tunnel study: $CO:CO_2$, $N_2O:CO_2$, $CH_4:CO_2$, $O_2:CO_2$ ratios, and the stable isotopes ^{13}C and ^{18}O in CO_2 and CO, Atmos. Chem. Phys., 14, 2105–2123, 2014.

Peltier, G., Cournac, L., Despax, V., Dimon, B., Fina, L., Genty, B., and Rumeau, D.: Carbonic anhydrase activity in leaves as measured in vivo by ^{18}O exchange between carbon dioxide and water, Planta, 196**,** 732-739, 1995.

Peng, T., Wang, H. C., and Huang, C.: Stable isotopic characteristic of Taiwan's precipitation: a case study of western Pacific monsoon region, Earth Planet. Sci. Lett., 289 (3–4), 357–366, 2010.

Peylin, P., Ciais, P., Denning, A. S., Tans, P. P., Berry, J. A., and White, J. W. C.: A 3-dimensional study of $\delta^{18}O$ in atmospheric CO_2: contribution of different land

Biogeosciences Discuss., doi:10.5194/bg-2016-106, 2016
Manuscript under review for journal Biogeosciences
Published: 18 April 2016

ecosystems, Tellus Series B—Chemical and Physical Meteorology, 51(3), 642–667, 1999.

Tans, P. P.,Berry, J. A., and Keeling, R. F.: Oceanic $^{13}C/^{12}C$ observations: A new window on ocean CO_2 uptake, Global Biogeochim. Cycles, 7(2) 353–368, 1993.

Thiemens, M. H., Chakraborty, S., Jackson, T. L.: Decadal $\Delta^{17}O$ record of tropospheric CO_2: Verification of a stratospheric component in the troposphere, J. Geophys. Res., 119, 6221–6229, 2014.

Wang, Z., Schauble, E. A., and Eiler, J. M.: Equilibrium thermodynamics of multiply substituted isotopologues of molecular gases, Geochim. Cosmochim. Acta, 68(23), 4779–4797, 2004.

Welp, L. R., Keeling, R. F., Meijer, H. A. J., Bollenbacher, A. F., Piper, S. C., Yoshimura, K., Francey, R. J., Allison, C. E., and Wahlen, M.: Interannual variability in the oxygen isotopes of atmospheric CO_2 driven by El Nino, Nature, 477, 579-582, 2011.

Yakir, D., and Wang, X. F.: Fluxes of CO_2 and water between terrestrial vegetation and the atmosphere estimated from isotope measurements, Nature, 380, 515-517, 1996.

Ye, F., Deng, W., Xie, L., Wei, G., and Jia, G.: Surface water $\delta^{18}O$ in the marginal China seas and its hydrological implications. Estuarine, Coastal and Shelf Science 147, 25-31, 2014.

Yeung, L. Y. et al.: Large and unexpected enrichment in stratospheric $^{16}O^{13}C^{18}O$ and its meredional variation, Proc. Nat. Acad. Sci. USA, 106(28), 11496-11501, 2009.

Yeung, L. Y., Ash, J. L., and Young, E. D.: Biological signatures in clumped isotopes of O_2, Science 348, 431–434, 2015.

Zhang, J., P. Quay, D., and Wilbur, D. O.: Carbon isotope fractionation during gas-water exchange and dissolution of CO_2, Geochim. Cosmochim. Acta., doi:10.1016/0016-7037(95)91550-d, 1995.

Biogeosciences Discuss., doi:10.5194/bg-2016-106, 2016
Manuscript under review for journal Biogeosciences
Published: 18 April 2016

Figures

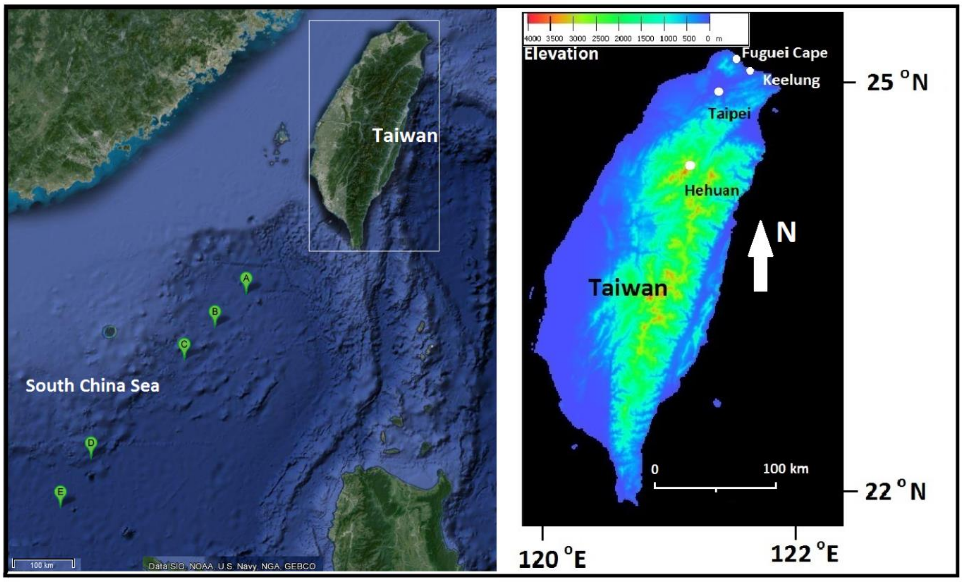

Figure 1. Map of Taiwan and South China Sea with the locations of air sampling. Marine air CO_2 sampling stations (A to E) in the South China Sea are shown on the left. Fuguei Cape and Keelung are two coastal stations, urban site (Roosevelt Road) and grassland (National Taiwan University Campus) are located at the centre of Taipei City and sub-urban site (Academia Sinica Campus) at the outskirt of the city and Hehuan is a high mountain station (~3000 m a.s.l.); all are shown on the right.

Biogeosciences Discuss., doi:10.5194/bg-2016-106, 2016
Manuscript under review for journal Biogeosciences
Published: 18 April 2016

Biogeosciences
Discussions
Open Access

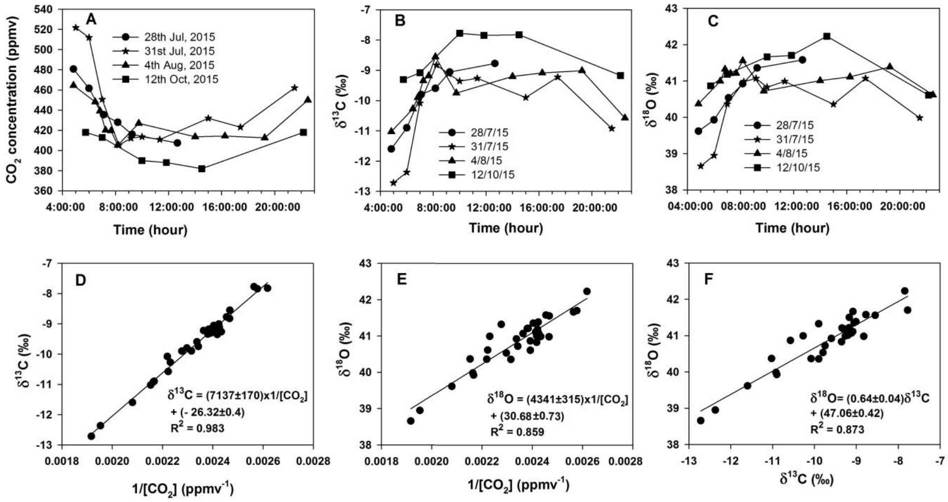

Figure 2. Top panels show the diurnal variation of (A) concentration, (B) $\delta^{13}C$, and (C) $\delta^{18}O$ of CO_2 sampled in the greenhouse. Bottom panels are the Keeling plots for (D) $\delta^{13}C$ and (E) $\delta^{18}O$ and (F) scatter plot of $\delta^{13}C$ and $\delta^{18}O$ to show their covariance.

Biogeosciences Discuss., doi:10.5194/bg-2016-106, 2016
Manuscript under review for journal Biogeosciences
Published: 18 April 2016

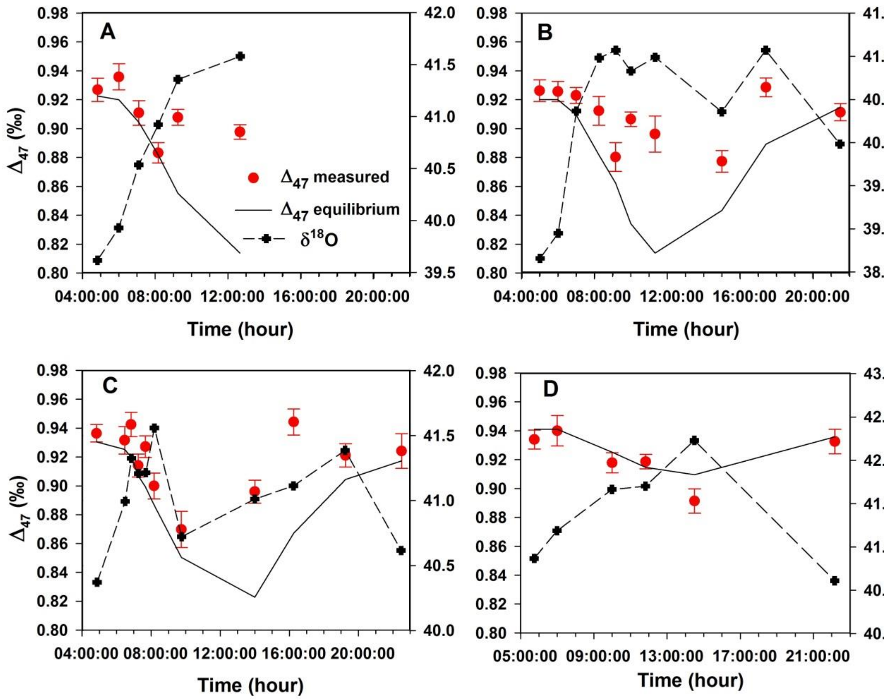

Figure 3. Diurnal variation of the Δ_{47} and $\delta^{18}O$ values in the greenhouse for samples collected on four days of 2015: (A) 28th July, (B) 31st July, (C) 4th August, and (D) 12th October. The first three days (A-C) were bright sunny days and the last one (D) on a cloudy day with covered rooftop (see texts for details). The error bars are 1 standard error associated with the measurements.

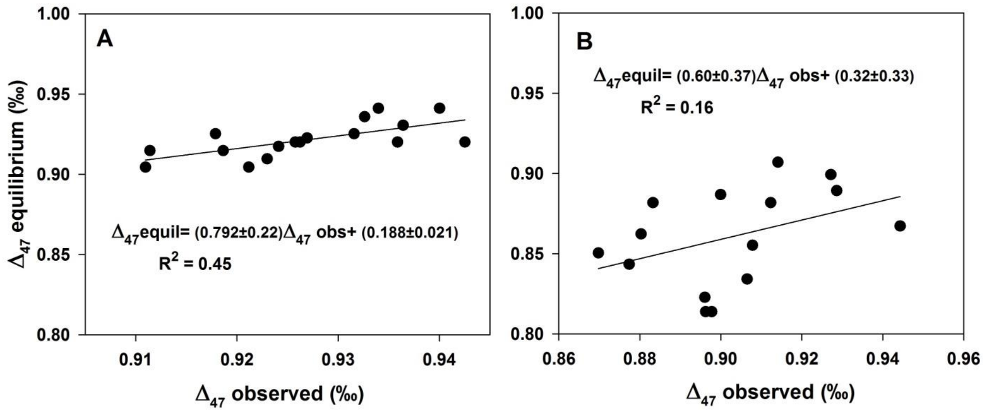

Figure 4. Correlation between the observed and thermodynamic equilibrium Δ_{47} values for greenhouse CO_2 samples collected when (A) photosynthesis is weak and respiration is strong and (B) photosynthesis is strong and respiration is weak.

Biogeosciences Discuss., doi:10.5194/bg-2016-106, 2016
Manuscript under review for journal Biogeosciences
Published: 18 April 2016

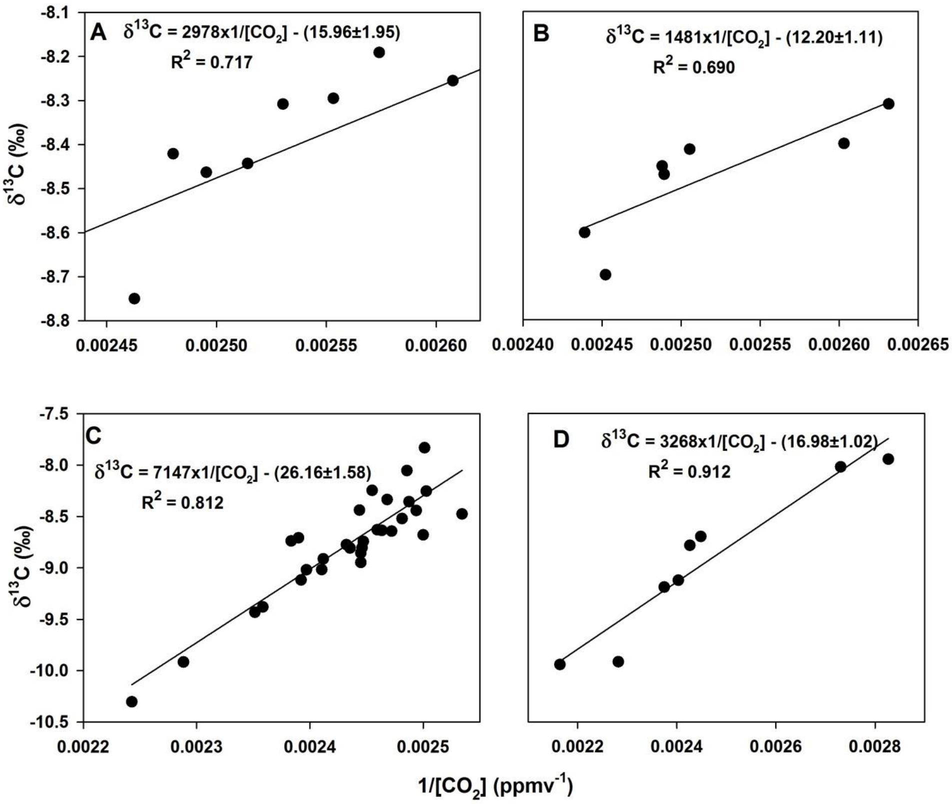

Figure 5. Carbon Keeling plots for atmospheric CO_2 collected at (A) South China Sea (B) Keelung and Fuguei Cape, (C) sub-urban station, Academia Sinica Campus, and (D) grassland, National Taiwan University. For more details about the sites, see the texts and Figure 1.

Biogeosciences Discuss., doi:10.5194/bg-2016-106, 2016
Manuscript under review for journal Biogeosciences
Published: 18 April 2016

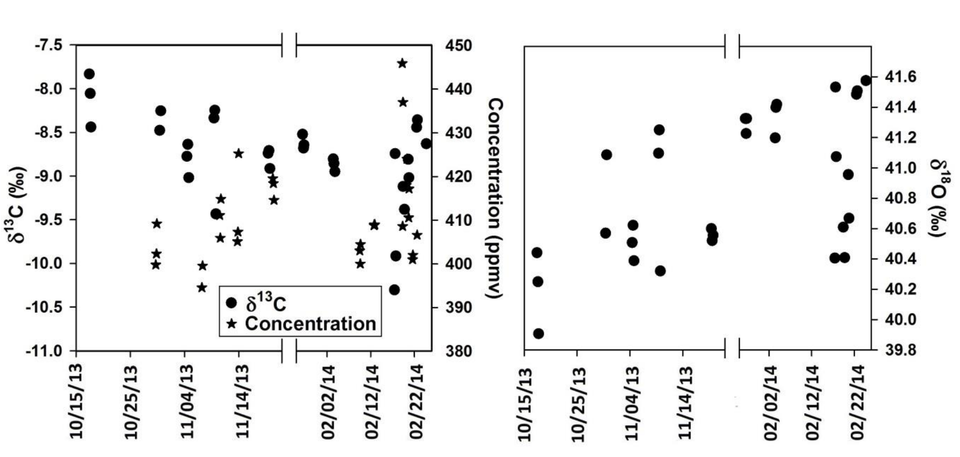

Figure 6. Time series of (A) concentration and stable carbon and (B) stable oxygen isotopes for CO_2 collected at Academia Sinica Campus.

Biogeosciences Discuss., doi:10.5194/bg-2016-106, 2016
Manuscript under review for journal Biogeosciences
Published: 18 April 2016

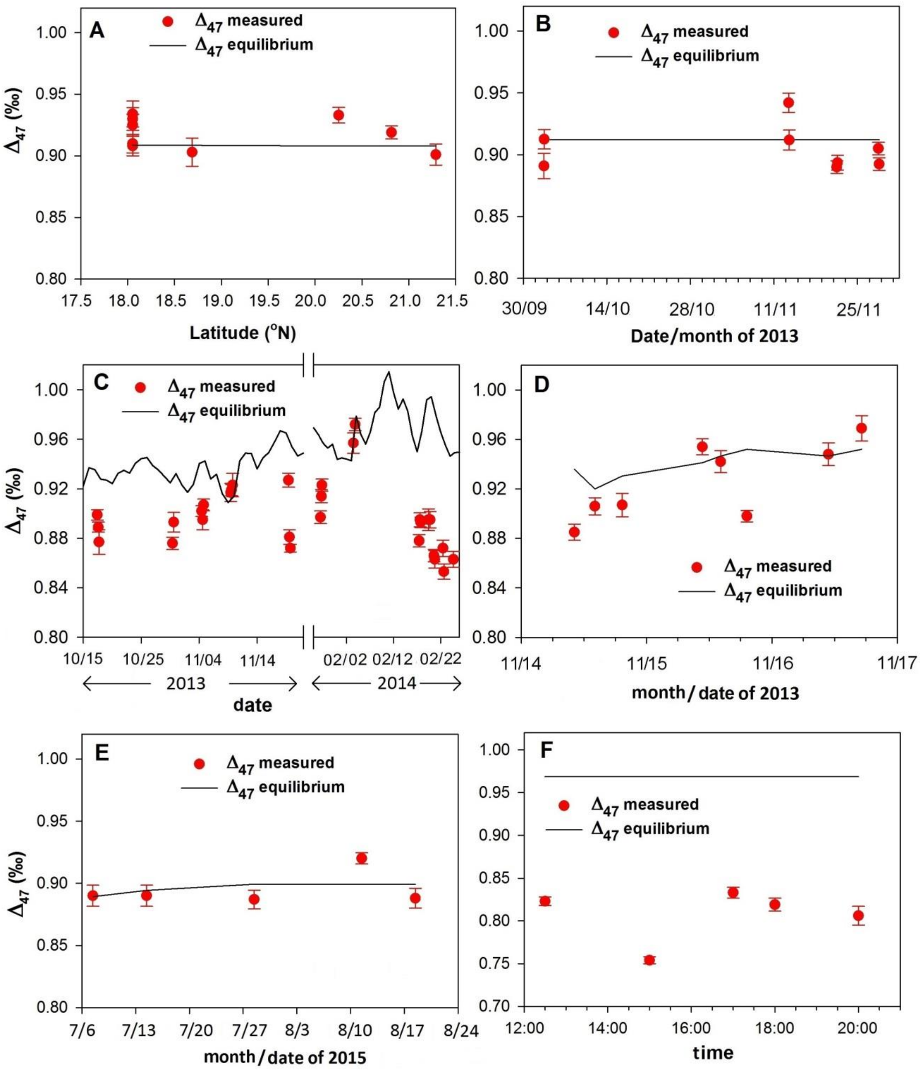

Figure 7. Δ_{47} values in the near surface atmospheric CO_2 from (A) South China Sea, (B) coastal stations (Keelung and Fuguei Cape), (C) sub-urban station (Academia Sinica campus), (D) grassland in the National Taiwan University campus, (E) forest site near the Academia Sinica Campus and (F) urban site (Roosevelt Road). The error bars are the 1 standard errors associated with the measurements. Lines show Δ_{47} values for the CO_2 in thermodynamic equilibrium at ambient temperatures.

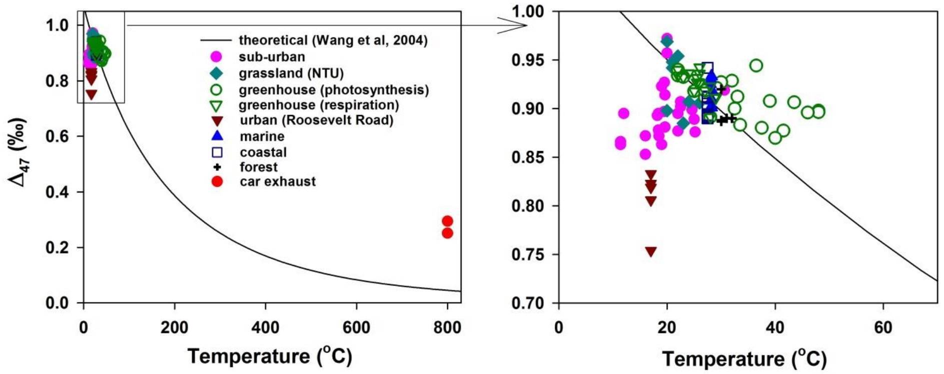

Figure 8. A summary of Δ_{47} values in near surface air CO_2 obtained at different environments and compared with the thermodynamic equilibrium values. Combustion temperature for car exhausts is assumed to be 800 °C (minimum value). Greenhouse CO_2 are divided into two categories: photosynthesis dominated (green open circle) and respiration dominated (green open triangle).

Biogeosciences Discuss., doi:10.5194/bg-2016-106, 2016
Manuscript under review for journal Biogeosciences
Published: 18 April 2016

Table 1. Reproducibility and precision of measurements for stable isotopes including Δ_{47} for IAEA NBS-19.

Sl. No.	$\delta^{13}C$(‰) (VPDB)	$\delta^{18}O$ (‰) (VPDB CO_2)	δ^{47}(‰)	Std. Err.	Δ_{47}(‰)	Std. Err.
1	2.02	-2.21	35.22	0.01	0.382	0.010
2	2.02	-2.11	35.54	0.02	0.394	0.012
3	2.02	-2.19	35.28	0.01	0.416	0.010
4	2.01	-2.28	35.15	0.01	0.408	0.011
5	2.00	-2.27	35.24	0.02	0.388	0.016
6	2.00	-2.16	35.27	0.02	0.370	0.013
7	2.02	-2.27	35.21	0.01	0.398	0.009
8	2.02	-2.20	36.48	0.01	0.363	0.008
9	2.01	-2.20	36.56	0.02	0.392	0.006
10	2.01	-2.15	36.46	0.01	0.399	0.012
11	2.01	-2.20	36.57	0.01	0.393	0.010
12	2.02	-2.21	36.32	0.01	0.387	0.009
13	2.01	-2.18	36.43	0.01	0.368	0.014
14	2.01	-2.16	35.81	0.01	0.379	0.010
15	2.00	-2.18	35.76	0.01	0.387	0.006
Average	2.01	-2.20	35.82		0.388	
Std. Dev.	0.01	0.05	0.58		0.014	

Biogeosciences Discuss., doi:10.5194/bg-2016-106, 2016
Manuscript under review for journal Biogeosciences
Published: 18 April 2016

Table 2. Diurnal variation of $\delta^{13}C$ and $\delta^{18}O$ and clumped isotopes (Δ_{47}) for greenhouse CO_2. Temperatures estimated using Δ_{47} values and actual air temperatures inside the greenhouse at the time of sampling are also presented.

Date	Time	Conc. (ppmv)	$\delta^{13}C$(‰) (VPDB)	$\delta^{18}O$(‰) (VSMOW)	δ^{47}(‰)	Std. err.	Δ_{47} (‰) (ARF)	Std. err.	Estimated temp. (°C)	Air temp. (°C)
7/28/2015	4:50	481	-11.60	39.61	6.99	0.02	0.927	0.016	24	25.5
	6:00	462	-10.90	39.92	8.16	0.02	0.936	0.018	21	26
	7:06	435	-9.80	40.54	9.71	0.02	0.911	0.017	28	29
	8:10	428	-9.60	40.92	10.38	0.02	0.883	0.014	33	33.5
	9:15	416	-9.06	41.36	11.30	0.01	0.908	0.011	24	39
	10:15	422	-9.55	40.82	NA	NA	NA	NA	NA	NA
	12:40	407	-8.77	41.58	11.75	0.01	0.898	0.010	27	48
7/31/2015	5:00	522	-12.72	38.66	5.10	0.01	0.926	0.015	24	26
	6:00	512	-12.37	38.95	5.94	0.01	0.926	0.014	25	26
	7:00	451	-10.08	40.36	9.39	0.02	0.923	0.011	25	28
	8:15	405	-8.82	40.98	11.25	0.02	0.912	0.020	28	33
	9:10	412	-9.12	41.07	11.26	0.02	0.880	0.020	34	37.5
	10:00	414	-9.35	40.83	11.52	0.01	0.906	0.010	23	43.5
	11:20	411	-9.26	40.99	11.12	0.02	0.896	0.025	31	48
	15:00	432	-9.90	40.36	9.55	0.02	0.877	0.015	34	41.5
	17:25	423	-9.22	41.07	12.48	0.02	0.929	0.013	25	32
	21:30	462	-10.92	39.99	7.90	0.01	0.911	0.012	28	27
8/4/2015	4:50	465	-11.03	40.37	8.41	0.01	0.936	0.012	23	24
	5:50	455	-10.82	40.26	NA	NA	NA	NA	NA	NA
	6:28	448	-10.27	41.00	10.01	0.02	0.931	0.017	24	25.5
	6:50	439	-9.90	41.32	10.10	0.02	0.942	0.009	22	26

Biogeosciences Discuss., doi:10.5194/bg-2016-106, 2016
Manuscript under review for journal Biogeosciences
Published: 18 April 2016

	7:15	420	-9.34	41.22	11.05	0.01	0.914	0.013	28	28.5
	7:40	419	-9.18	41.22	11.05	0.01	0.927	0.011	25	30
	8:10	405	-8.55	41.56	12.79	0.02	0.900	0.015	31	32.5
	9:45	427	-9.75	40.73	10.81	0.02	0.870	0.023	36	40
	14:00	414	-9.20	41.01	11.02	0.01	0.896	0.011	31	46
	16:15	414	-9.09	41.11	11.11	0.01	0.944	0.014	22	36.5
	19:15	413	-9.01	41.38	13.28	0.01	0.921	0.010	26	29.2
	22:30	450	-10.58	40.61	9.34	0.02	0.924	0.022	25	26.5
10/12/2015	5:45	418	-9.30	40.87	10.80	0.01	0.934	0.013	23	22
	7:00	413	-9.08	41.18	10.95	0.02	0.940	0.021	22	22
	10:00	390	-7.78	41.66	13.00	0.02	0.918	0.014	26	25
	11:50	388	-7.84	41.71	15.25	0.01	0.919	0.010	26	27
	14:30	382	-7.82	42.24	14.27	0.02	0.891	0.017	31	28
	20:10	418	-9.17	40.61	10.85	0.02	0.933	0.017	23	23

Table 3. Stable carbon and oxygen isotopic composition and clumped isotopes (Δ_{47}) for car exhaust CO_2. Temperatures estimated using Δ_{47} values and lowest possible combustion temperatures are given.

Car model	Conc. (ppm)	$\delta^{13}C$(‰) (VPDB)	$\delta^{18}O$(‰) (VSMOW)	δ^{47}(‰)	Std. err.	Δ_{47} (‰) (ARF)	Std. err.	Estimated temp. (°C)	Combustion temp. (°C)
Mazda 3000cc TRIBUTE	39400	-27.73	25.43	-22.20	0.01	0.251	0.013	300	800
Mitsubishi 2400cc New Outlander	39300	-27.67	25.27	-23.08	0.02	0.294	0.007	265	800
Average ± 1σ	39350±50	-27.70±0.03	25.35±0.07	-22.64±0.44		0.273±0.021		283±18	

Table 4. Stable isotopic composition including Δ_{47} for air CO_2 collected over South China Sea and two coastal stations (see Figure 1 for sampling locations). Temperatures estimated using Δ_{47} values and the sea surface temperatures at the time of samplings are also presented.

Marine air CO_2									
South China Sea									
Date time	Conc. (ppm)	$\delta^{13}C$(‰) (VPDB)	$\delta^{18}O$(‰) (VSMOW)	δ^{47}(‰)	Std. err.	Δ_{47} (‰) (ARF)	Std. err.	Estimated temp. (°C)	Sea surface temp. (°C)
10/15/2013 8:15 (A)*	403	-8.42	40.85	28.752	0.016	0.901	0.017	30	28.3
10/15/2013 13:15 (B)	400	-8.46	40.80	28.441	0.012	0.919	0.011	26	28.3
10/15/2013 18:00 (C)	406	-8.75	40.54	28.133	0.013	0.933	0.013	24	28.3
10/16/2013 7:00 (D)	391	-8.76	40.53	27.916	0.024	0.903	0.023	29	28.2
10/16/2013 12:05 (E)	397	-8.44	40.86	28.535	0.015	0.910	0.015	28	28.2
10/16/2013 14:00 (E)	391	-8.30	40.96	28.922	0.021	0.934	0.021	23	28.2
10/16/2013 17:20 (E)	395	-8.31	41.02	28.944	0.017	0.908	0.016	29	28.1
10/16/2013 20:20 (E)	388	-8.19	40.52	28.909	0.018	0.930	0.018	24	28.1
10/17/2013 8:40 (E)	383	-8.26	40.41	28.194	0.018	0.925	0.018	25	28.1
Average ± 1σ	395±7	-8.43±0.19	40.72±0.20	28.52±0.36		0.918±0.012		27±2	28.2±0.1
Keelung									
10/03/2013 11:30	380	-8.31	40.31	28.053	0.020	0.896	0.021	31	27.5
10/03/2013 12:30	384	-8.40	40.92	29.089	0.017	0.917	0.016	27	27.5

Biogeosciences Discuss., doi:10.5194/bg-2016-106, 2016
Manuscript under review for journal Biogeosciences
Published: 18 April 2016

11/13/2013 11:00	401	-8.45	40.62	29.645	0.015	0.946	0.016	21	27.5
11/21/2013 12:30		-8.47	40.78	29.866	0.017	0.890	0.010	32	27.5
11/28/2013 12:00	410	-8.60	40.21	28.992	0.011	0.908	0.010	28	27.5
Average ± 1σ	394±12	-8.45±0.09	40.57±0.26	29.12±0.63		0.911±0.020		28±4	27.5
Fuguei Cape									
11/13/2013 13:30	401	-8.47	40.76	29.56	0.02	0.916	0.016	27	27.5
11/21/2013 15:30	399	-8.41	40.89	29.37	0.01	0.880	0.012	34	27.5
11/28/2013 15:00	407	-8.70	41.16	30.11	0.01	0.886	0.010	33	27.5
Average ± 1σ	402±3	-8.53±0.12	40.94±0.16	29.68±0.29		0.894±0.015		31±3	27.5

*Sampling Stations (see Figure 1 for locations in South China Sea)

Table 5. Stable isotopic composition including clumped isotopes (Δ_{47}) for air CO_2 collected in urban and sub-urban stations, grassland, forest and high mountain environments. Temperatures estimated using Δ_{47} values and air temperatures are also presented.

Urban CO_2: Roosevelt Road, Taipei City										
Date	Time	Conc. (ppm)	δ^{13}C(‰) (VPDB)	δ^{18}O(‰) (VSMOW)	δ^{47}(‰)	Std. err.	Δ_{47} (‰) (ARF)	Std. err.	Estimated temp. (°C)	Air temp. (°C)
12/30/ 2015	12:30	510	-10.41	40.00	25.26	0.014	0.823	0.010	46	20
	15:00	478	-11.50	38.49	22.63	0.012	0.754	0.008	62	19.5
	17:00	461	-9.69	40.70	26.74	0.017	0.833	0.013	44	17
	18:00	594	-12.30	38.14	21.56	0.014	0.819	0.015	47	16
	20:00	457	-11.34	39.24	23.61	0.022	0.806	0.022	50	15
Average±1σ		500±50	-11.05±0.90	39.31±0.94	23.96±1.84		0.807±0.028		50±6	17±2

Biogeosciences Discuss., doi:10.5194/bg-2016-106, 2016
Manuscript under review for journal Biogeosciences
Published: 18 April 2016

Sub-urban air CO_2									
Academia Sinica Campus									
Date time	Conc. (ppm)	$\delta^{13}C$(‰) (VPDB)	$\delta^{18}O$(‰) (VSMOW)	δ^{47}(‰)	Std. err.	Δ_{47} (‰) (ARF)	Std. err.	Estimated temp. (°C)	Air temp (°C)
10/17/2013 10:00	400	-7.83	40.44	28.47	0.015	0.899	0.008	30	25
10/17/2013 14:30	402	-8.05	40.25	28.07	0.017	0.889	0.008	32	25
10/17/2013 17:20	409	-8.44	39.90	27.26	0.019	0.877	0.020	34	22
10/30/2013 10:00	395	-8.48	40.57	28.47	0.012	0.876	0.010	35	25.2
10/30/2013 14:30	400	-8.25	41.08	29.03	0.016	0.893	0.016	31	27.4
11/04/2013 10:30	411	-8.78	40.51	28.67	0.011	0.902	0.009	29	22.5
11/04/2013 14:30	406	-8.64	40.62	28.97	0.017	0.895	0.016	31	22
11/04/2013 18:30	415	-9.02	40.38	28.33	0.013	0.907	0.009	28	22.5
11/09/2013 10:30	405	-8.34	41.09	29.79	0.019	0.917	0.015	27	28.5
11/09/2013 14:00	407	-8.25	41.25	30.63	0.015	0.919	0.009	26	30.6
11/09/2013 18:30	425	-9.43	40.32	27.49	0.020	0.923	0.019	25	28
11/19/2013 10:00	419	-8.74	40.60	29.27	0.012	0.927	0.011	25	19.5
11/19/2013 14:00	418	-8.71	40.52	29.59	0.019	0.881	0.012	33	19.6
11/19/2013 18:00	414	-8.91	40.56	28.58	0.012	0.872	0.006	35	18.5
01/27/2014 10:30	403	-8.52	41.32	30.13	0.008	0.897	0.010	30	19.2
01/27/2014 15:20	400	-8.68	41.23	30.03	0.011	0.914	0.010	27	19.6
01/27/2014 18:00	404	-8.64	41.32	29.29	0.017	0.923	0.010	25	18.5
02/03/2014 11:00	408	-8.80	41.20	29.67	0.015	0.957	0.017	19	24.5
02/03/2014 14:30	409	-8.86	41.39	NA		NA			
02/03/2014 19:30	409	-8.95	41.41	30.57	0.011	0.972	0.010	16	19.3

Biogeosciences Discuss., doi:10.5194/bg-2016-106, 2016
Manuscript under review for journal Biogeosciences
Published: 18 April 2016

02/17/2014 10:30	445	-10.30	40.40	27.60	0.016	0.878	0.010	34	22.4
02/17/2014 14:30	408	-8.74	41.53	30.58	0.014	0.895	0.011	31	25
02/17/2014 18:30	437	-9.92	41.07	28.49	0.012	0.893	0.008	31	22
02/19/2014 10:00	418	-9.12	40.61	29.12	0.020	0.895	0.018	31	13.3
02/19/2014 18:00	424	-9.38	40.40	28.49	0.020	0.895	0.013	31	12.4
02/20/2014 14:30	410	-8.81	40.96	29.68	0.023	0.866	0.010	37	12.9
02/20/2014 18:00	417	-9.02	40.66	29.59	0.018	0.863	0.014	37	12.5
02/22/2014 12:15	401	-8.44	41.49	30.63	0.013	0.872	0.013	35	17.5
02/22/2014 17:00	402	-8.36	41.51	30.63	0.013	0.853	0.012	40	17.1
02/24/2014 17:30	406	-8.63	41.57	30.70	0.014	0.863	0.013	37	22
Average ± 1σ	411±11	-8.78±0.50	40.87±0.46	29.23±1.00		0.897±0.027		30±5	21±5
Grassland: NTU Campus									
11/14/2013 10:10	353	-7.95	40.96	30.18	0.02	0.885	0.013	33	23
11/14/2013 14:05	366	-8.02	41.31	30.79	0.01	0.906	0.014	29	26
11/14/2013 19:20	462	-9.94	38.33	25.64	0.02	0.907	0.019	29	24
11/15/2013 10:40	416	-9.12	39.42	29.51	0.01	0.954	0.013	20	22
11/15/2013 14:10	421	-9.19	39.36	29.78	0.02	0.942	0.018	22	21
11/15/2013 19:12	438	-9.92	38.28	28.08	0.04	0.989	0.009	13	20
11/16/2013 10:50	412	-8.78	40.03	28.54	0.02	0.948	0.018	21	21
11/16/2013 17:10	408	-8.70	40.26	26.06	0.02	0.969	0.021	17	20
Average ± 1σ	409±33	-8.95±0.70	39.74±1.00	28.57±1.77		0.937±0.030		23±6	22±2
Forest site near Academia Sinica Campus									
07/07/2015 10:30	411	-9.07	41.43	11.54	0.01	0.890	0.017	32	32
07/14/2015 10:30	458	-10.43	39.74	9.01	0.02	0.890	0.017	32	31
07/28/2015 10:40	441	-9.99	40.86	10.07	0.02	0.887	0.015	32	30
08/11/2015 10:40	448	-10.46	40.09	9.50	0.01	0.920	0.009	26	30

Biogeosciences Discuss., doi:10.5194/bg-2016-106, 2016
Manuscript under review for journal Biogeosciences
Published: 18 April 2016

08/18/2015 10:30	433	-9.99	39.80	8.99	0.02	0.888	0.016	32	30
Average ± 1σ	438±16	-9.99 ±0.50	40.39±0.66	9.82±0.94		0.895±0.012		31±2	31±1
High mountain: Hehuan									
10/09/2013 13:20	364	-8.21	40.89	28.79	0.02	0.895	0.016	31	10
10/09/2013 17:00	NA	-8.25	40.28	28.41	0.01	0.914	0.014	27	10
Average ± 1σ	364	-8.23 ±0.02	40.59±0.30	28.60±0.19		0.904±0.009		30±2	10